Naval Research Laboratory

Washington, DC 20375-5000

NRL Memorandum Report 6662

Non-Maxwellian Electron Distribution Functions in Z-Pinch Plasmas

P. E. PULSIFER AND K. G. WHITNEY

Radiation Hydrodynamics Branch
Plasma Physics Division

July 27, 1990

This work was supported by the Defense Nuclear Agency under Project Task Code and Title, RL RA/Advanced Technology Development, Work Unit Code and Title, 00079, Advanced Technology Development, MIPR No. 89-565.

REPORT DOCUMENTATION PAGE

Form Approved
OMB No. 0704-0188

1. AGENCY USE ONLY (Leave blank)	2. REPORT DATE	3. REPORT TYPE AND DATES COVERED
	1990 July 27	Interim

4. TITLE AND SUBTITLE
Non-Maxwellian Electron Distribution Functions in Z-Pinch Plasmas

5. FUNDING NUMBERS
PE - 62715H
WU - DN880-191

6. AUTHOR(S)
P. E. Pulsifer and K. G. Whitney

7. PERFORMING ORGANIZATION NAME(S) AND ADDRESS(ES)
Naval Research Laboratory
Radiation Hydrodynamics Branch
Code 4720
Washington, D.C. 20375-5000

8. PERFORMING ORGANIZATION REPORT NUMBER
NRL Memorandum Report 6662

9. SPONSORING/MONITORING AGENCY NAME(S) AND ADDRESS(ES)
Defense Nuclear Agency
RAEV
Washington, D.C. 20305

10. SPONSORING/MONITORING AGENCY REPORT NUMBER

11. SUPPLEMENTARY NOTES
This research was sponsored by the Defense Nuclear Agency under Project Task Code and Title, RL RA/Advanced Technology Development, Work Unit Code and Title, 00079, Advanced Technology Development, MIPR No. 89-565.

12a. DISTRIBUTION/AVAILABILITY STATEMENT
Approved for public release; distribution unlimited.

12b. DISTRIBUTION CODE
Statement A

13. ABSTRACT *(Maximum 200 words)*

The heating and cooling of a z-pinch electron distribution is studied using the Fokker-Planck equation. Included in the analysis are the usual Fokker-Planck term for distant small-angle electron-electron collisions, a semi-empirical term representing inelastic charge-conserving collisions, ohmic heating by the electric field acting on the current, and compressional heating or cooling. Ions are represented as heavy, highly-charged Maxwellian particles, and electron-ion collisions are given in terms of a Coulomb collision frequency. In deriving the Fokker-Planck equation, a first-order Cartesian tensor expansion is performed in a local coordinate system which is spatially uniform and moving with the fluid. The first-order (vector) term in the expansion is assumed to equilibrate much faster than the zero-order (scalar) term. Under some conditions, the electron distribution function has an analytic self-similar solution. A numerical time-dependent solution is also obtained, through an implicit finite-differencing scheme. Advantages of a time-dependent model are noted. The behavior of the electron distribution function and conductivity are demonstrated for different parameters. Production of runaway electrons with perpendicular electric and magnetic fields is discussed.

14. SUBJECT TERMS
Z-Pinch Dynamics, Kinetic Theory, Conductivity, Non-Equilibrium Distributions, Runaway Electrons

15. NUMBER OF PAGES
58

16. PRICE CODE

17. SECURITY CLASSIFICATION OF REPORT	18. SECURITY CLASSIFICATION OF THIS PAGE	19. SECURITY CLASSIFICATION OF ABSTRACT	20. LIMITATION OF ABSTRACT
UNCLASSIFIED	UNCLASSIFIED	UNCLASSIFIED	SAR

NSN 7540-01-280-5500

Standard Form 298 (Rev 2-89)
Prescribed by ANSI Std Z39-18
298-102

CONTENTS

I.	Introduction	1
II.	Physical Picture	3
III.	Basic Equations	5
IV.	Analytical Results	15
V.	Numerical Method of Solution	24
VI.	Numerical Results	28
VII.	Appendix I	30
VIII.	Appendix II	33
IX.	Appendix III	35
X.	Appendix IV	38
XI.	References	39
DISTRIBUTION LIST		51

NON-MAXWELLIAN ELECTRON DISTRIBUTION FUNCTIONS IN Z-PINCH PLASMAS

1. Introduction

A knowledge of the electron distribution function is necessary for accurate determination of z-pinch fluid and radiation dynamics. Distribution function dynamics underlie the magnetohydrodynamic behavior of the pinch, affecting implosion time and implosion energy as well as the coupling efficiency between generator and load. The radiation yield of the pinch may depend sensitively on these factors, which determine the energy input to the pinch and thus influence the energy spectrum of the radiation; in addition, the flux of high-energy electrons is an immediate influence on the radiation spectrum due to collisional excitation in the pinch.

Study of the electron distribution function is the only way to investigate non-thermal phenomena like runaways and the plasma-wave turbulence of anomalous resistivity. Runaway electrons have been observed in z-pinch experiments,[1] despite the strong toroidal magnetic fields at the pinch edge, and may be an important factor in both fluid and radiation dynamics, reducing coupling by providing an alternative current path and contributing to radiative instabilities, since they are associated with "bright spots".[1] But the production and propagation of z-pinch runaways is not well understood at this time. Anomalous resistivity and the limiting of electron drift velocity due to particle-wave interactions play an important role in the pinch, by both increasing the rate of diffusion of current and fields into the plasma (thereby altering the force structure and so the implosion dynamics) and by increasing the energy input to the plasma following its assembly on axis. Information is now needed on how to control these factors for appropriate radiation yields in a variety of pinch parameters and materials.

The shape of the high-energy distribution of electrons plays an important role in determining kilovolt x-ray conversion efficiencies in z-pinches. Still, the literature provides an unclear picture of the effects that different interactions in a z-pinch have on this part of the distribution, since these effects depend diversely on the state of the plasma and on the rate of energy input or output from it. Under various conditions the tail of the distribution may be enhanced or depleted, may be extended or may acquire a high energy plateau.

Manuscript approved February 27, 1990.

Most prior studies of the Fokker-Planck equation have been related to tokomacs or inertial-confinement fusion. In the former case, the electric and magnetic fields are taken to be parallel and runaway rates are computed for those conditions. In the latter case, cross-field transport is computed, but with the assumption of weak magnetic fields. Usually, the Fokker-Planck equation is linearized about a Maxwell-Boltzmann equilibrium distribution. An earlier z-pinch study, related to this one, investigated equilibrium (time-independent) solutions to the nonlinear Fokker-Planck equation in a z-pinch.[2] These earlier approaches have limited usefulness for studying dynamic z-pinch implosions, which are characterized by rapid change and strong, perpendicular, spatially varying electric and magnetic fields.

The principal effects that must be accounted for in a kinetic, Fokker-Planck description of the electron distribution function dynamics are: (1) the strong electric field heating (ohmic heating); (2) the equally strong electron-electron elastic collisions; and (3) the diffusion-like electron-plasma wave interactions that determine the strength of the instability-driven plasma turbulence. In this report a basic theory is set up which is suitable for treating all three of these effects under the dynamically evolving conditions found in a z-pinch implosion. However, only the effects of ohmic heating and electron-electron collisions will be studied in this report; the theory of the turbulence interaction and its contribution to the picture presented here will be discussed in a later report. A time-dependent theory is essential because the different processes, with different timescales, change in relative importance during the course of the implosion, and because some of the phenomena studied, like runaways, are essentially non-equilibrium in nature. Also, with the time-dependent theory it is possible to continually assess the accuracy of the approximations used on physical grounds; this provides a check on the results.

The Maxwell-Boltzmann equilibrium distribution is produced by small-angle electron-electron collisions, and this equilibrium will be maintained on their (< 0.1 ns) time scale. Heating and cooling processes acting preferentially in one energy range will disrupt this equilibrium. Because the electron collision time decreases with velocity, return to equilibrium is especially slow in the distribution tail. The heating and cooling processes considered here include ohmic heating, compression, and radiation. Ohmic heating results from electric field acceleration of electrons. Compressional heating or cooling is calculated from spatial gradients in the fluid velocity, which are supplied as input (e.g., from MHD z-

pinch simulations). Radiation losses can be calculated from inelastic electron-ion collisions, assuming an optically thin medium.

This report forms a compendium of analytic results, drawn from many sources, which are relevant to z-pinch kinetics. It draws connections to other work, particularly on laser heating by inverse bremsstrahlung and on electron distributions in tokomacs. Analytic results are obtained whenever possible, and individual effects on the electron distribution are analyzed in depth. In particular, expressions for the conductivity and runaway production rates are given. Finally, a numerical solution is obtained to the fully non-linear time-dependent Fokker-Planck equation. This numerical solution will later be used in conjunction with an MHD code to estimate the magnitude of non-thermal effects in actual z-pinch implosions.

2. Physical Picture

The system is composed of electrons, of mass m, and various ion species α, each with mass $M_\alpha \gg m$, charge Z_α and density n_α. The mean charge number is $Z = n_e/n_i\,(\approx 10)$, where $n_e = \sum_\alpha n_\alpha Z_\alpha$ and $n_i = \sum_\alpha n_\alpha$. The electrons are described by a distribution function $f(r, v, t)$. The ions are assumed to maintain a Maxwell-Boltzmann distribution. Electrons are subject to both electrostatic forces $m\vec{a}_L = Ze\vec{E}$ and magnetic forces $m\vec{\omega} = (Ze/c)\vec{B}$; the fields, E and B, are locally uniform in time and space. (The electric field E should not be confused with the average electron energy $\langle E \rangle$).

The collision frequency for elastic Coulomb scattering (Rutherford frequency) of a particle of species α moving with velocity v_α through a number density n_β of species β particles is

$$\nu_{\alpha\beta}(v_\alpha) = \left[n_\beta v_\alpha (\pi \ell_\alpha^2)\right]\left[(Z_\alpha Z_\beta)^2 \log \Lambda_\alpha\right], \tag{1}$$

where $\ell_\alpha = 2e^2/m_\alpha v_\alpha^2$, called the Landau length, is the distance of closest approach of the scattering particle and the threshold for large-angle collisions; and the Coulomb logarithm is given by

$$\log \Lambda_\alpha = \log\left[\frac{3}{2\sqrt{\pi}} \frac{(kT)^{3/2}}{Z_\alpha e^3 \sqrt{n_\alpha}}\right] \tag{2}$$

The first bracketed term in eq. (1) is the cross-sectional flux (the number of particles

per second passing through particle α's path), and the second term is the Coulomb scattering factor, giving the interaction strength between the two scattering particles.[†] Substituting for ℓ_α in eq. (1) and simplifying gives

$$\nu_{\alpha\beta} = \frac{4\pi e^4}{m_\alpha^2} \frac{Z_\alpha^2 Z_\beta^2 n_\beta}{v_\alpha^3} \log \Lambda_\alpha. \tag{3}$$

The "temperature" of the non-equilibrium system is defined to be proportional to the average energy in the system:

$$kT \equiv \frac{1}{q}\langle E \rangle. \tag{4}$$

Different proportionality constants are used by different authors; the choice consistent with the expression for temperature in an equilibrium (3D) system, however, is $q = 3/2$. The thermal velocity is also defined in terms of the average system energy:

$$v_{th} = \sqrt{\frac{2\langle E \rangle}{m}}. \tag{5}$$

This is related to the temperature with the constant q: if $q = 3/2$, $v_{th} = \sqrt{3kT/m}$. The electron-electron collision frequency at the thermal velocity will be denoted

$$\nu_R \equiv \nu_{ee}(v_{th}). \tag{6}$$

The geometry of the system is that of a z-pinch, cylindrically symmetric about the pinch axis. The system is assumed to be spatially uniform in the $\hat{\phi}$ and $\hat{z}$ directions; important radial gradients do exist, however. Radial variations are included in the model by dividing the pinch into concentric, spatially uniform thin cells, with time-varying inner and outer radii and a mean velocity $\vec{V}(r,t)$. The electron distribution function $f(v,t)$ is then

[†] Other illustrative forms for $\nu_{\alpha\beta}$ can be obtained, such as, for atomic physics applications,

$$\nu_{\alpha\beta} = n_\beta v_\alpha (\pi a_0^2) \left(\frac{Z_\alpha Z_\beta}{m v_\alpha^2 / 4Ry} \right)^2 \log \Lambda_\alpha,$$

where a_0 is the Bohr radius and $Ry = e^2/2a_0$ is the Rydberg energy; or, for high-energy (non-relativistic) physics, a_0 can be replaced by $r_e = e^2/mc^2$, the classical electron radius, and $2Ry$ by $m_e c^2$, the electron rest-mass energy.

to be found within the reference frame of each dynamically evolving cell. This approach includes the important effects (compressional heating or cooling) of bulk electron motion on the electron dynamics, without requiring that the Fokker-Planck kinetic equation be solved in configuration space.

3. Basic Equations

In this section the model kinetic (Boltzmann) equation will be presented, an expansion will be performed and the first-order terms obtained, and a zero-order nonlinear Fokker-Planck equation will be obtained for analysis.

Relative to a stationary observer, the electron distribution function satisfies the (collisional) Boltzmann equation[3]

$$\frac{\partial f}{\partial t} + \vec{v}_L \cdot \vec{\nabla} f + (\vec{a}_L + \vec{v}_L \times \vec{\omega}) \cdot \vec{\nabla}_{v_L} f = \left(\frac{\delta f}{\delta t}\right)_C . \tag{7}$$

where v_L is the particle velocity in the stationary "lab" frame, $\vec{a}_L = Ze\vec{E}/m$ and $\vec{\omega} = (Ze/mc)\vec{B}$. In each z-pinch cell, the system is moving with a time-dependent average fluid velocity $V(r,t)$. The particle velocity and electric-field acceleration in this reference frame are

$$\vec{v}(\vec{r}, \vec{v}_L, t) = \vec{v}_L - \vec{V}(\vec{r}, t) \tag{8}$$

$$\vec{a} = \frac{Ze}{m}\vec{E} + \vec{V} \times \vec{\omega} - \frac{d\vec{V}}{dt}; \tag{9}$$

the comoving time derivative

$$d/dt = \partial/\partial t + \vec{V} \cdot \vec{\nabla} \tag{10}$$

gives changes with respect to the moving frame. Derivatives in the moving frame are given by

$$\frac{\partial f(\vec{v})}{\partial t} = \frac{\partial f}{\partial t} + \frac{\partial f}{\partial \vec{v}} \frac{\partial \vec{v}}{\partial t} = \frac{\partial f}{\partial t} - \frac{\partial \vec{V}}{\partial t} \cdot \vec{\nabla}_v f$$

$$\vec{\nabla} f(\vec{r}, \vec{v}, t) = \vec{\nabla} f - (\vec{\nabla}\vec{V}) \cdot \vec{\nabla}_v f. \tag{11}$$

Therefore, in a reference frame moving with velocity V, the Boltzmann equation becomes[4]

$$\frac{df}{dt} + \vec{v} \cdot \vec{\nabla} f + \left[\vec{a} + \vec{v} \times \vec{\omega}\right] \cdot \vec{\nabla}_v f - \vec{v} \cdot \vec{\nabla}\vec{V} \cdot \vec{\nabla}_v f = C_{el} + C_{inel} \tag{12}$$

The last term on the left-hand side vanishes if the mean velocity $\vec{V}$ is spatially uniform; it is through this term that compressional effects enter. Collisions are represented on the right-hand side of the Boltzmann equation: C_{el} gives the effects of elastic collisions, a Fokker-Planck term in this model, and C_{inel} describes inelastic processes. These terms will be discussed in detail later.

Cartesian tensor expansion

Instead of being a scalar function of the vector position and velocity variables, the distribution function $f(\vec{x},\vec{v},t)$ can be expressed in terms of scalar, vector, tensor, etc. functions of scalar position and velocity variables.[4] If only first-order terms are retained, the expansion reads

$$f(\vec{x},\vec{v},t) \approx f_0(x,v) + \frac{1}{v}\left[\vec{v}\cdot\vec{f}_1(x,v)\right] \tag{13}$$

This first-order expansion is sufficient to determine averages of any quantity that is a linear function of the scalar v and vector $\vec{v}$. It can always be used if $\vec{f}_1$ (and higher-order terms) is sufficiently small, and with certain geometries it can be used regardless of the magnitude of f_1. The different terms of the expansion, when known, can be used to compute average values such as the density and temperature. For example, the average value of a function $\phi(v)$ is

$$\langle\phi\rangle = \frac{4\pi}{n}\int_0^\infty \phi f_0 v^2\, dv \tag{14}$$

and the average value of a function $\psi(\vec{v})$ which is linearly dependent on the vector $\vec{v}$ is

$$\langle\psi\rangle = \frac{4\pi}{3n}\int_0^\infty \psi(\vec{f}_1(v))v^2\, dv. \tag{15}$$

In particular, the mean number density $n(x) = \langle 1\rangle$ and current density $\vec{j} = \langle en\vec{v}\rangle$ are

$$n(x) = 4\pi\int_0^\infty v^2 f_0(x,v)\, dv. \tag{16}$$

$$\vec{j}(x) = \frac{4\pi}{3}\epsilon\int_0^\infty v^3 f_1(x,v)\, dv. \tag{17}$$

When the expansion of eq. (13) is substituted into the Boltzmann equation, eq. (12), and the various angular moments are taken (this procedure is illustrated in Appendix II),

the result is[4]:

$$\frac{df_0}{dt} + \frac{v}{3}\vec{\nabla}\cdot\vec{f}_1 - \vec{\nabla}\cdot\vec{V}\frac{v}{3}\frac{\partial f_0}{\partial v} + \frac{1}{3v^2}\frac{\partial}{\partial v}\left[v^2\vec{a}\cdot\vec{f}_1\right] = C_{FP} + C^* \tag{18a}$$

$$\frac{d\vec{f}_1}{dt} + v\vec{\nabla}f_0 + \vec{a}\frac{\partial f_0}{\partial v} + \vec{\omega}\times\vec{f}_1 - \vec{\nabla}\vec{V}\cdot\vec{f}_1$$

$$- [\vec{\nabla}\vec{V} + \vec{\nabla}\vec{V}^T + \mathbf{I_2}\vec{\nabla}\cdot\vec{V}]\cdot\frac{v^2}{5}\frac{\partial}{\partial v}\left(\frac{\vec{f}_1}{v}\right) = \vec{C}_1 \tag{18b}$$

where C_{FP} and $\vec{C}_1$ come from C_{el}, and C^* comes from C_{inel}, on the right-hand-side of eq. (7). There is no contribution to the $\vec{f}_1$ equation from inelastic collisions because these collisions are assumed to be isotropic and so do no change the average momentum of the system.

The physical content of eqs. (18) is fairly clear, if one bears in mind that f_0 describes the particle density and f_1 its current. Eq. (18a) describes the change in time of f_0 resulting from the net current inflow (the $\vec{\nabla}\cdot\vec{f}_1$ and $\vec{\nabla}\cdot\vec{V}$ terms), work done on the current by the electric field ($\vec{a}\cdot\vec{f}_1$), and collisions, both elastic (C_{FP}) and inelastic (C^*). Eq. (18b) gives changes in $\vec{f}_1$ corresponding to flows driven by density gradients (the $\vec{\nabla}f_0$ and $\vec{\nabla}\vec{V}$ terms) and by the electric field, which moves nonuniformities in $f(\vec{v})$ through velocity space (the $\vec{a}\,\partial f_0/\partial v$ term). The effect of these driving factors is modified by the deflecting nature of the magnetic field ($\vec{\omega}\times\vec{f}_1$), and by elastic collisions ($\vec{C}_1$).

Eqs. (18) are rigorous, except for the neglect of higher-order expansion terms like f_2 in eq. (18b). The procedure now is to solve eq. (18b) for $\vec{f}_1$ under physically reasonable simplifying assumptions, and then to substitute the resulting expression for $\vec{a}\cdot\vec{f}_1$ into eq. (18a) to get an equation that can be numerically solved for f_0. An immediate simplification comes if we ignore the (assumed) weak effects of the currents that are driven by density and temperature gradients, i.e., only gradients in the fluid velocity $\vec{V}$ will be retained. Then $\vec{\nabla}\cdot\vec{f}_1 = 0$ and $\vec{\nabla}f_0 = 0$, and eqs. (18) may be summarized as follows:

$$\frac{df_0}{dt} = C_{FP} + C^* + C_C + C_a \tag{19a}$$

$$\frac{d\vec{f}_1}{dt} + \vec{a}\frac{\partial f_0}{\partial v} + \vec{\omega}\times\vec{f}_1 = \vec{T} + \vec{C}_1 \tag{19b}$$

where C_{FP} describes elastic collisions, C^* describes inelastic collisions, C_C and $\vec{T}$ contain

compressional effects, and C_a is due to electric-field heating. These terms are discussed in detail below.

Elastic collisions

The elastic collision terms in eqs. (19) come from the expansion of the C_{el} term in eq. (12), which includes contributions from all particle species: $C_{el} = \sum_\alpha C_{el}^{(\alpha)}$. The zero-order term C_{FP} describes energy exchange in collisions, while the first-order term describes momentum transfer, and so has no contributions from like-particle collisions. If $F_{\alpha i}$ is the i-th order term in the expansion of the distribution function for species α, the general expressions are[4,5] [The C_{FP} equation is derived in Appendix I]:

$$C_{FP}^{(\alpha)} = \frac{Y_{e\alpha}}{v^2}\frac{\partial}{\partial v}\left[\frac{m}{M_\alpha} f_0 I_0^0 + \frac{v}{3}\frac{\partial f_0}{\partial v}\left(I_2^0 + J_{-1}^0\right)\right] \tag{20a}$$

$$\begin{aligned}\vec{C}_1^{(\alpha)} = \frac{Y_{e\alpha}}{v^3}\Bigg\{ & \frac{v^2}{3}\frac{\partial^2 \vec{f}_1}{\partial v^2}(I_2^0 + J_{-1}^0) + \frac{v}{3}\frac{\partial \vec{f}_1}{\partial v}\left(\frac{3m}{M} I_0^0 - I_2^0 + 2J_{-1}^0\right) + \frac{1}{3}\vec{f}_1(-3I_0^0 + I_2^0 - 2J_{-1}^0) \\ & + 4\pi v^3 \frac{m}{M}(\vec{f}_1 F_{\alpha 0} + \vec{F}_{\alpha 1} f_0) + \frac{v^2}{5}\frac{\partial^2 f_0}{\partial v^2}(\vec{I}_3^1 + \vec{J}_{-2}^1) \\ & + \frac{v}{15}\frac{\partial f_0}{\partial v}\left[-3\vec{I}_3^1 + \left(7 - 5\frac{m}{M}\right)\vec{J}_{-2}^1 + \left(-5 + 10\frac{m}{M}\right)\vec{I}_1^1\right]\Bigg\}\end{aligned} \tag{20b}$$

with the definitions

$$Y_{\alpha\beta} = 4\pi \left(Z_\alpha Z_\beta e^2/m_\alpha\right)^2 \log\Lambda_\alpha = \frac{\nu_{\alpha\beta}}{n_\beta} v_\alpha^3 \tag{21}$$

$$I_j^i(v) = \frac{4\pi}{v^j}\int_0^v F_{\alpha i}(V) V^{j+2}\, dV \tag{22}$$

$$J_j^i(v) = \frac{4\pi}{v^j}\int_v^\infty F_{\alpha i}(V) V^{j+2}\, dV \tag{23}$$

These expressions can be simplified.

Electron-electron collisions dominate in C_{FP} because of the extreme mass difference between electrons and ions (just as there is very little collisional interaction between a basketball and a Mack truck, which have about the same mass ratio). The electron-ion term C_{FP}^i) is proportional to m/M_i and so is ignored. With only electron-electron collisions included, the term C_{FP} in eq. (20a) becomes

$$C_{FP} = 4\pi\frac{Y_{ee}}{v^2}\frac{\partial}{\partial v}\left[f_0\int_0^v f_0(v') v'^2\, dv' + \frac{v}{3}\frac{\partial f_0}{\partial v}\left(\frac{1}{v^2}\int_0^v f_0(v') v'^4\, dv' + v\int_v^\infty f_0(v') v'\, dv'\right)\right] \tag{24}$$

In the $\vec{C}_1$ term it is ion-electron collisions that are important, because no momentum is exchanged in collisions between like particles. In eq. (20b), the large ion mass allows us to approximate $\vec{F}_{i1} \approx 0$ – the ions acquire no motion from electron-ion collisions. If the ions are assumed to be in a spherically symmetric Maxwellian distribution, then $\vec{C}_1$ simplifies considerably. The integrals involved in I_j^i and J_j^i then become functions of the error function $\Phi(v\sqrt{M/2kT})$ and its derivatives[4], and because of the relatively large ion mass only the large-argument limit of these functions need be considered. In this limit, $J_{-1}^0 \approx 0$; $I_0^0 \approx n_i$; and $i_2^0 \approx 3n_i kT/Mv^2$, and if terms proportional to m/M are again dropped, eq. (20b) becomes (see eq. (3))

$$\vec{C}_1 \approx -\nu_{ei}\vec{f}_1 \tag{25}$$

Essentially, these approximations assume that the ions affect but are not affected by the electrons. Ion equilibrium is plausible because of the large ion-ion collision rate ($\nu_{ii}/\nu_{ee} \approx Z^4$) as well as because of the large ion mass.

Because electron-ion collisions are much more frequent than electron-electron collisions ($\nu_{ei}/\nu_{ee} = Z$), and because f_1 changes on the timescale of ν_{ei} while f_0 changes like ν_{ee}, then f_1 equilibrates much faster than f_0. This ordering of time development will be used later. The electron-ion collisions represented by ν_{ei} damp any increase in f_1 and cause a drag on electron flow; the decrease of ν_{ei} with increasing v results in high-energy electrons becoming "runaways".

Inelastic collisions

The inelastic collision term C^* in eq. (19a) can be obtained by requiring conservation of particle number in collisions. Inelastic collisions transfer energy from electrons to ions, exciting the ions to a higher energy level. The ions are assumed to immediately re-radiate this energy through the optically thin medium, so that electron-ion collisions alone do not significantly change the ion level populations. The minimum free-electron energy to excite a transition from level a to level b is the excitation energy ϵ_{ab}. The number of ion levels contributing significantly to the electron kinetics is generally small, of the order of 10.

Since ionization and recombination are not considered here, the number of ions and free electrons is conserved in inelastic collisions. Collisional losses are described, then, by

subtracting electrons from a higher energy region of the distribution function and replacing them at a lower energy region. Each of the possible inelastic scattering processes can be numbered by an index j; if the collision frequency for process j is ν_j^*, then the collision term is of the form

$$C^* = \sum_j \left[-\nu_j^*(\epsilon) f_0(\epsilon) + \sqrt{\frac{\epsilon + \epsilon_j}{\epsilon}}\, \nu_j^*(\epsilon + \epsilon_j) f_0(\epsilon + \epsilon_j) \right] \tag{26}$$

The first term in the sum represents the rate of scattering to lower energy of particles with energy ϵ, while the second term represents the influx of particles to energy ϵ from collisions involving higher-energy particles. $C^*(\epsilon)$ thus gives the net rate of increase in the distribution function at energy ϵ due to all inelastic scattering processes. The factor $\sqrt{(\epsilon + \epsilon_j)/\epsilon}$ makes allowance for the greater phase-space volume available at the energy $\epsilon + \epsilon_j$ from which the electrons scatter to energy ϵ: the number of electrons scattered between energy ϵ and $\epsilon + \epsilon_j$ is always $\nu^*(\epsilon) f_0(\epsilon)\, 4\pi\sqrt{\epsilon}\, d\epsilon$.

The inelastic collision frequency for an electron (velocity v) to excite an ion from level a (density $f_a n_i$) to level b is

$$\nu_{ab}^* = f_a n_i \left[\pi a_0^2 \frac{\Omega_{ab}(\epsilon)/g_a}{\epsilon/Ry}\, \theta(\epsilon - \epsilon_{ab}) \right] v. \tag{27}$$

The quantity in brackets above is the inelastic cross-section, which is expressed in terms of the measured dimensionless collision strength $\Omega_{ab}(\epsilon)$. The multiplicity of level a is g_a. The Heaviside step function θ relects the energy threshold for the transition. A plot of typical collision strengths for argon is given in fig. (1); typically, Ω_{ab} is of order 1, varying little over the energy range. The ratio of the inelastic collision frequency to the electron-electron collision frequency ν_{ee} is

$$\frac{\nu_{ab}^*}{\nu_{ee}} = \frac{f_a \Omega_{ab}}{g_a} \left(\frac{\epsilon/Ry}{4Z \log \Lambda} \right) \theta(\epsilon - \epsilon_{ab}). \tag{28}$$

This is generally small; since the only terms not of order one are Z and $\log \Lambda$, which are each near 10, an effect of perhaps a few percent for each transition might be anticipated from inelastic collisions. Because the ratio increases with ϵ, however, greater effects should appear in the tail of the distribution, in particular at energies greater than Z times the

thermal energy. Also, since the inelastic term is a sum, the cumulative effect of inelastic collisions could be quite significant, if many important transitions are available to the system.

Compressional heating

The compressional term in eq. (19a) comes directly from eq. (18a):

$$C_C = \left(\vec{\nabla} \cdot \vec{V}\right) \frac{v}{3} \frac{\partial f_0}{\partial v}. \tag{29}$$

This describes changes in the distribution function f_0 caused by a plasma compression or expansion which is reflected in the nonuniform fluid velocity V. Taking moments of C_C reveals that this term conserves neither local particle density nor average energy:

$$\left(\frac{dn}{dt}\right)_C = -n\vec{\nabla} \cdot \vec{V} \tag{30}$$

$$\left(\frac{d\langle E\rangle}{dt}\right)_C = -\langle E\rangle \frac{5}{3}\vec{\nabla} \cdot \vec{V} \tag{31}$$

The change in density in eq. (30) is just that resulting from the continuity equation for compression or expansion of a uniform-density flow of electrons. The change in energy density in eq. (31) is caused by PdV work: the pressure $P = 2\langle E\rangle/3$, and integrating $\vec{\nabla} \cdot \vec{V}$ shows it to be the time rate of change of the system volume.

The effect of compression on the first-order equation, eq. (19b), comes from

$$\vec{T} \equiv \vec{\nabla}\vec{V} \cdot \vec{f}_1 + [\vec{\nabla}\vec{V} + \vec{\nabla}\vec{V}^T + \mathbf{I_2}\vec{\nabla} \cdot \vec{V}] \cdot \frac{v^2}{5} \frac{\partial}{\partial v}\left(\frac{\vec{f}_1}{v}\right), \tag{32}$$

where $\mathbf{I_2}$ denotes the 3×3 unit tensor. This term is not simple; in a cylindrical coordinate system and with $\vec{V}$ in the $\hat{r}$ direction only, the components of $\vec{T}$ are

$$\begin{cases} T^{(r)} = \dfrac{1}{5}\left[2\dfrac{\partial V}{\partial r} - \dfrac{1}{r}V\right] f_1^{(r)} + \dfrac{v}{5}\left[3\dfrac{\partial V}{\partial r} + \dfrac{1}{r}V\right] \dfrac{\partial f_1^{(r)}}{\partial v} \\ T^{(\phi)} = \dfrac{1}{5}\left[-\dfrac{\partial V}{\partial r} + \dfrac{2}{r}V\right] f_1^{(\phi)} + \dfrac{v}{5}\left[\dfrac{\partial V}{\partial r} + \dfrac{3}{r}V\right] \dfrac{\partial f_1^{(\phi)}}{\partial v} \\ T^{(z)} = \dfrac{1}{5}\left[-\dfrac{\partial V}{\partial r} - \dfrac{1}{r}V\right] f_1^{(z)} + \dfrac{v}{5}\left[\dfrac{\partial V}{\partial r} + \dfrac{1}{r}V\right] \dfrac{\partial f_1^{(z)}}{\partial v} \end{cases}$$

Since there is no shear in the cylindrically-symmetric flow, no mixing of the different components of $\vec{f}_1$ occurs as a result of the compression. The effects included in $\vec{T}$ are small, since they are second order in the small quantities $\vec{f}_1$ and $\vec{\nabla}\vec{V}$. They modify the response of the fluid to the applied electric field due to a changing plasma density, and should be small compared to ν_{ei}. In this treatment, therefore, we take $\vec{T} = 0$.

Electric field – Ohmic Heating

Work done on the electrons by the electric field shows up in the zero-order distribution function through the term C_a in eq. (19a):

$$C_a = -\frac{1}{3v^2}\frac{\partial}{\partial v}\left[v^2 \vec{a}\cdot\vec{f}_1\right]. \tag{33}$$

When this energy is distributed throughout the plasma by electron-ion collisions, it causes the bulk heating which is ohmic heating. The magnetic field is important in ohmic heating, since is alters the electron trajectory. It will be seen that this shifts the heating to lower-energy electrons; the heat then must be transferred to high-energy electrons by elastic scattering, whose strength decreases with energy.

To find C_a, eq. (19b) must be solved for $\vec{a}\cdot\vec{f}_1$. This is straightforward in the center-of-mass system. With eq. (25) for $\vec{C}_1$ and $\vec{T} = 0$, eq. (19b) is

$$\frac{d\vec{f}_1}{dt} + \vec{\omega}\times\vec{f}_1 = -\nu_{ei} f_1 - \vec{a}\frac{\partial f_0}{\partial v} \tag{34}$$

An equilibrium solution is sought for $\vec{f}_1$ ($\vec{f}_1$ reaches equilibrium on the timescale of ν_{ei}, which is Z times faster than the ν_{ee} timescale of f_0). It can readily be verified that if $d\vec{f}_1/dt = 0$, the equilibrium $\vec{f}_1$ is

$$\vec{f}_1 = \frac{1}{\omega^2+\nu_{ei}^2}\left[\vec{\omega}\times\vec{a} - \frac{\vec{\omega}\cdot\vec{a}}{\nu_{ei}}\vec{\omega} - \nu_{ei}\vec{a}\right]\frac{\partial f_0}{\partial v}. \tag{35}$$

Thus

$$\vec{a}\cdot\vec{f}_1 = -\frac{a^2 + (\vec{a}\cdot\vec{\omega}/\nu_{ei})^2}{\nu_{ei}(1+\omega^2/\nu_{ei}^2)}\frac{\partial f_0}{\partial v} \tag{36}$$

When the electric field acts parallel to the magnetic field, C_a is independent of ω, as it should be. When the electric and magnetic forces are perpendicular, as in the Bennett z-pinch, then $\vec{a}\cdot\vec{\omega} = 0$, and the ohmic heating term C_a becomes

$$C_a = C_{EB} \equiv \frac{1}{3v^2}\frac{\partial}{\partial v}\left[v^2\frac{a^2}{\nu_{ei}(1+\omega^2/\nu_{ei}^2)}\frac{\partial f_0}{\partial v}\right]. \tag{37}$$

Normalization

For ease of computation, it is useful to express the quantities given above in terms of dimensionless variables, using characteristic velocity, time and space variables for normalization. A dimensionless velocity representation is presented and then used as a stepping stone to the dimensionless energy representation used in the remainder of this work.

Characteristic magnitudes used in scaling are: for time, the thermal electron-electron collision time $\tau_R = \nu_R^{-1}$ (see eq. (6)); for length, the mean electron separation $n^{-1/3}$; for velocity or energy, the thermal velocity v_{th} (see eq. (5)). The characteristic electric field is the Dreicer field[10] $E_D = mv_{th}\nu_R/e$, which is the electric field that would accelerate an electron from rest to the thermal velocity in one thermal collision time. The characteristic magnetic field has a cyclotron frequency of ν_R: $B_D = mc\nu_R/e$.

The dimensionless velocity ξ is defined with respect to the thermal velocity (eq. (5)):

$$\xi \equiv \frac{v}{v_{th}}. \tag{38}$$

It can be seen from eq. (16) that $f_0(v)$ has dimensions of $\left[\frac{\text{density}}{(\text{velocity})^3}\right]$. Therefore the dimensionless distribution function $\bar{f}_0$ is:

$$\bar{f}_0 = \frac{v_{th}^3}{n} f_0(v) \tag{39}$$

The function $\bar{f}_0$ is a probability distribution whose average density (eq. (16)) is normalized to one. To make eq. (19a) dimensionless, both sides are multiplied by $v_{th}^3\tau_R/n$. The new elastic collision term is then

$$\bar{C}_{FP} = \frac{v_{th}^2\tau_R}{n} C_{FP} = \frac{1}{\xi^2}\frac{\partial}{\partial\xi}\left\{\bar{f}_0(\xi)\bar{N}(\xi) + \bar{D}(\xi)\frac{\partial\bar{f}_0}{\partial\xi}\right\}, \tag{40}$$

where

$$\bar{N}(\xi) \equiv 4\pi\int_0^\xi \bar{f}_0(\xi')\xi'^2\, d\xi' \tag{41}$$

$$\bar{D}(\xi) \equiv \frac{4\pi}{3}\left[\frac{1}{\xi}\int_0^\xi \bar{f}_0(\xi')\xi'^4\, d\xi' + \xi^2\int_\xi^\infty \bar{f}_0(\xi')\xi'\, d\xi'\right]. \tag{42}$$

The dimensionless inelastic-collision term $\bar{C}^*$ is just eq. (26) with the collision frequency ν_j replaced by the dimensionless frequency

$$\bar{\nu}_j^*(\xi) = \nu_j^*(\xi)/\nu_R(\xi). \tag{43}$$

Since the compression term C_C does not conserve density, a term proportional to dn/dt results on substituting the dimensionless distribution function $\bar{f}_0$ into eq. (19a). If this term is evaluated from eq. (30), it can be combined with C_C and the normalized kinetic equation will then maintain a constant normalization. The true density must then be computed from the integral of eq. (30). The dimensionless compression term is then

$$\bar{C}_C = \frac{v_{th}^2 \tau_R}{n} C_C - \frac{1}{n}\frac{dn}{d\tau}\bar{f}_0 = \vec{\nabla}\cdot\vec{V}\frac{\tau_R}{3\xi^2}\frac{\partial}{\partial\xi}\left(\xi^3\bar{f}_0\right) \tag{44}$$

The dimensionless ohmic heating term is

$$\bar{C}_{EB} = \frac{\alpha}{\xi^2}\frac{d\bar{\zeta}(\xi)}{d\xi} \tag{45}$$

where

$$\alpha = Z\mathcal{E}^2 \tag{46}$$

$$\bar{\zeta}(\xi) = \frac{1}{3Z^2}\frac{\xi^5}{1+\Omega^2\xi^6/Z^2}. \tag{47}$$

and the dimensionless electric and magnetic field variables are $\mathcal{E} = E/E_D$ and $\Omega = \omega/\nu_R$. The velocity dependence of the collision frequency $\nu_{ei}(v)$ has been used:

$$\frac{\nu_{ei}}{\nu_R} = \frac{n_i Y_{ei}}{n_e Y_{ee}}\xi^{-3} = Z\xi^{-3}, \tag{48}$$

In terms of dimensionless velocity variables, the kinetic equation, eq. (19a) is

$$\frac{d\bar{f}_0}{d\tau} = \frac{1}{\xi^2}\frac{\partial}{\partial\xi}\left\{\left[\bar{N}(\xi) + \frac{\xi^3}{3}\tau_R\vec{\nabla}\cdot\vec{V}\right]\bar{f}_0(\xi) + \left[\bar{D}(\xi) + \alpha\bar{\zeta}(\xi)\right]\frac{\partial f_0}{\partial\xi}\right\} + \bar{C}'. \tag{49}$$

The dimensionless energy variable is defined in terms of the temperature (see eq. (4)):

$$\epsilon = \frac{mv^2/2}{kT} = q\xi^2. \tag{50}$$

Important relations between the dimensionless velocity and energy variables are

$$\xi = \sqrt{\epsilon/q}, \quad \frac{d}{d\xi} = 2\sqrt{q\epsilon}\frac{d}{d\epsilon}, \quad d\xi = \frac{1}{2\sqrt{q\epsilon}}d\epsilon. \tag{51}$$

In terms of the dimensionless energy, and with the following definitions (new definitions from ϵ-dependent functions are denoted by a new argument):

$$N(\epsilon) \equiv 4\pi \int_0^\epsilon d\epsilon' \sqrt{\epsilon'}\, f_0(\epsilon') \tag{52}$$

$$D(\epsilon) \equiv 4\pi \frac{2}{3}\left[\int_0^\epsilon d\epsilon' f_0(\epsilon')\epsilon'^{3/2} + \epsilon^{3/2}\int_\epsilon^\infty d\epsilon' f_0(\epsilon')\right] \tag{53}$$

$$\alpha = Z\mathcal{E}^2 = \frac{Ze^2}{2m\langle E\rangle \nu_R^2}E^2 \tag{54a}$$

$$\zeta(\epsilon) = \frac{4}{3Z^2\sqrt{q}}\frac{\epsilon^3}{1+\Omega^2\epsilon^3/Z^2q^3} \tag{54b}$$

$$C^*(\epsilon) = \sum_{a\ states}\left\{-\frac{\nu_{ab}^*(\epsilon)}{\nu_R}f_0(\epsilon) + \sqrt{\frac{\epsilon+\epsilon_{ab}}{\epsilon}}\,\frac{\nu_{ab}^*(\epsilon+\epsilon_{ab})}{\nu_R}f_0(\epsilon+\epsilon_{ab})\right\} \tag{55}$$

$$\nu_{ab}'(\epsilon) = \frac{\nu_{ab}^*(v)}{\nu_R} = \frac{q^{3/2}\alpha_{FS}^{-1}}{2Z\log\Lambda}\left[\frac{f_a\Omega_{ab}(\epsilon)}{g_a}\right]\left[\frac{kT}{mc^2\sqrt{\epsilon}}\right]\theta(\epsilon-\epsilon_{ab}) \tag{56}$$

where $\alpha_{FS} \approx 1/137$ is the fine-structure constant, the kinetic equation, eq. (19a) becomes:

$$\frac{df_0}{d\tau} = \frac{1}{\sqrt{\epsilon}}\frac{\partial}{\partial\epsilon}\left\{\left[N(\epsilon) + \frac{2\tau_R}{3r}\frac{\partial(rV)}{\partial r}\epsilon^{3/2}\right]f_0(\epsilon) + [D(\epsilon)+\alpha\zeta(\epsilon)]\frac{\partial f_0}{\partial\epsilon}\right\} + C^*(\epsilon) \tag{57}$$

This form of the Fokker-Planck equation will be the basis for the following analysis.

4. Analytical Results

In this section, analytical expressions are found for the conductivity both parallel to and perpendicular to the magnetic field; different expressions are presented for studying "runaway" in a magnetic field, self-similar solutions are found for the time-development of the distribution function, and the effects of ohmic heating, compression, and inelastic collisions are studied.

Conductivity

The conductivity of the plasma can be computed by using the definition of the conductivity tensor σ:

$$\vec{j} = \sigma \cdot \vec{E} \tag{58}$$

with the current $\vec{j}$ computed from the distribution function according to eq. (17).

With cylindrical symmetry and a nonzero magnetic field, the conductivity tensor has two different components, a parallel conductivity $\sigma_\parallel$ along the electric field, and a perpendicular (or Hall) conductivity $\sigma_\perp$ perpendicular to the electric field. The parallel conductivity is easily obtained from eq. (36):

$$j_\parallel = \frac{\vec{a}\cdot\vec{j}}{|a|} = -\frac{4\pi e^2}{3mn_iY_{ei}}E\int_0^\infty \frac{v^6}{1+v^6\omega^2/n_i^2Y_{ei}^2}\frac{\partial f_0}{\partial v}\,dv. \qquad (59))$$

Identifying terms, and expressing the integral in the dimensionless energy form, the parallel conductivity is

$$\sigma_\parallel = -\frac{Z\nu_R}{3}\left(\frac{\omega_p}{\omega}\right)^2\int_0^\infty \frac{\epsilon^3}{Z^2q^3/\Omega^2+\epsilon^3}\frac{\partial f_0}{\partial\epsilon}\,d\epsilon \qquad (60)$$

where $\omega_p \equiv \sqrt{4\pi ne^2/m}$ is the electron plasma frequency, and $\Omega = \omega/\nu_R$, as defined in the text. The Hall conductivity can be obtained directly from eq. (34), from which follows (with $\vec{a}\cdot\vec{\omega} = 0$)

$$\vec{a}\times\vec{f}_1 = -\frac{\vec{\omega}}{\nu_{ei}}\left(\vec{a}\cdot\vec{f}_1\right) \qquad (61)$$

This gives the perpendicular distribution in terms of the parallel one, so that

$$\sigma_\perp = \frac{1}{3q^{3/2}}\frac{\omega_p^2}{\omega}\int_0^\infty \frac{\epsilon^{9/2}}{Z^2q^3/\Omega^2+\epsilon^3}\frac{\partial f_0}{\partial\epsilon}\,d\epsilon. \qquad (62)$$

Both the magnetic field and the temperature affect the conductivity, as does the electric field because of its effect on the distribution function. In the strong magnetic field limit ($\Omega \gg Zq^{3/2}$) the conductivity reduces to

$$\sigma_\parallel(\omega\to\infty) \approx \frac{Z\nu_R}{3}\left(\frac{\omega_p}{\omega}\right)^2 f_0(\epsilon=0) \to 0 \qquad (63a)$$

$$\sigma_\perp(\omega\to\infty) \approx -\frac{n}{2q^{3/2}}\frac{\omega_p^2}{\omega} \to 0. \qquad (63b)$$

In the weak magnetic field limit, the conductivity becomes

$$\sigma_\parallel(\omega\to 0) \approx -\frac{\omega_p^2}{q^3Z\nu_R}\int_0^\infty \epsilon^2 f_0(\epsilon)\,d\epsilon \qquad (64a)$$

$$\sigma_\perp(\omega\to 0) \approx \omega\frac{1}{3Z^2q^{9/2}}\left(\frac{\omega_p}{\nu_R}\right)^2\int_0^\infty \epsilon^{7/2} f_0(\epsilon)\,d\epsilon \to 0. \qquad (64b)$$

These agree, in the appropriate limit, with accepted expressions for the static magneto-conductivity[9].

At low temperatures, the runaway effect dominates, and raising the temperature decreases collisions and increases conductivity. At high temperatures, however, the magnetic field dominates, and collisions increase conductivity by breaking the magnetic confinement; thus, increasing the temperature and decreasing collisions actually decreases the conductivity. This behavior is shown in fig. (2), where $\sigma_\parallel$ (calculated with $f_0(\epsilon)$ a Maxwellian) is plotted as a function of temperature.

The current in the pinch is not parallel to the electric field. Instead, from eq. (58),

$$\vec{j} = \left[\hat{r}\sigma_\perp + \hat{z}\sigma_\parallel\right] E, \tag{65}$$

which is a conical flow of current at an angle $\theta_j = \tan^{-1}(\sigma_\parallel/\sigma_\perp)$ from the pinch axis. In the actual pinch, this non-axial current will probably be of short duration; as with the Hall effect in a conductor, a radial charge-separation electric field will quickly develop in the pinch which will direct the current back onto the axis. The true parallel conductivity is here taken to be $\sigma_\parallel$.

As an alternative to the above calculation, the parallel conductivity in eq. (60) could also have been obtained by computing the heating rate due to C_{EB}. The ohmic heating is just equal to $\sigma_\parallel E^2$, and the coefficient of E^2 in the resulting expression is just $\sigma_\parallel$. These two methods are equivalent and self-consistent.

Runaway electrons

The Coulomb collision rate decreases with relative energy (see eq. (3)); this implies that particles with large enough kinetic energy are not significantly affected by collisions. Electrons with sufficient energy become runaways, and behave almost as free particles accelerated by the electric field. With no magnetic field, runaway electrons are those with a velocity greater than the critical velocity[10] $v_c \approx v_{th}\sqrt{3E_D/qE}$. (Dreicer's "critical field" E_c is E_D/q in the present notation). The critical velocity v_c is independent of v_{th} (since $\nu_R \propto v_{th}^{-3}$); as the system is heated and v_{th} increases, an increasing number of electrons have velocities above v_c and thus run away.

When inelastic collisions and a magnetic field are present, the situation is more complicated. Inelastic collisions may inhibit runaways by providing an energy sink and so preventing sufficient acceleration. A strong perpendicular magnetic field acts to stop transport of charged particles on any length scale larger than the cyclotron radius $r_c = 2.3845\sqrt{K}/B$ cm (where K is the electron energy in eV and B is the magnetic field in Gauss). If this distance is smaller than the anode-cathode gap, the electrons can only flow from anode to cathode if collisions break the magnetic field localization. Thus, for strong magnetic fields, energetic electrons are more efficiently trapped by the field and freely-accelerating runaways are eliminated. Still, even in this case energetic electrons can play an important role in the system, and can acquire significant directionality from drifts or collisions.

It is clear that with the z-pinch, unlike with the tokomac, one cannot define an arbitrary energy cutoff beyond which electrons behave as if freely accelerated by the electric field. The appropriate definition of "runaway" depends on the application. Finite-size effects can be estimated using the mean free path and the physical dimensions of the system. The rate at which high-energy electrons are produced can be found by defining a *velocity threshold* (e.g., v_c) and calculating the electron flux past this threshold. Beams of electrons can be found by looking for peaks in the distribution function. Because of the bending effect of the magnetic field, peaks in the distribution function rarely correspond to monodirectional beams; there is usually comparable electron flux both parallel and antiparallel to the electric field. Directionality can be checked using the first term in the expansion: $f_0(v) + f_1(v)$ is the directional distribution function.

Anisotropy in the electron velocity distribution shows up in $\vec{f}_1$, which can be considered a "current distribution function" (see eq. (17)). A nonzero $f_1(\epsilon)$ indicates a directed streaming at energy ϵ. In the presence of a magnetic field, $\vec{f}_1$ is not parallel to the electric field $\vec{a}$, though it is always perpendicular to the magnetic field $\vec{\omega}$ (this follows from eq. (34), since $\vec{a} \cdot \vec{\omega} = 0$). The magnetic field induces an $\vec{E} \times \vec{B}$ drift in the electron motion, while electron-ion collisions interrupt the drift motion and allow the current to flow along $\vec{E}$. In a z-pinch geometry $\vec{\omega}$ in the $\hat{\phi}$ direction and $\vec{E}$ and $\vec{f}_1$ in the $\hat{r}$-$\hat{z}$ plane,

the angle $\theta(\epsilon)$ between $\vec{f}_1(\epsilon)$ and $\vec{a}$ is given by

$$\tan\theta = \frac{|\vec{a}\times\vec{f}_1|}{\vec{a}\cdot\vec{f}_1} = -\frac{\omega}{\nu_{ei}} = -\frac{\Omega}{Z}\left(\frac{\epsilon}{q}\right)^{3/2}. \tag{66}$$

In the real pinch the electric field is composed of an applied field in the $\hat{z}$ direction, and an induced, r-dependent component in the radial direction to inhibit charge collection on the edge of the pinch (see the discussion following eq. (65)). The flux of electrons at a given energy, $\vec{f}_1(\epsilon)$, will also generally have a radial component, which tends to prevent focused beams and, if the magnetic field is strong enough that collisional electrons flow radially, to promote radial isotropy in the plasma. Electron-ion collisions, by interfering with this magnetic field-induced mixing, tend to promote beam-type anisotropy – just the opposite of the situation with no magnetic field.

The magnitude of the electron directionality can be found from the full distribution function. Parallel to the electric field, the distribution function is $f_0(\epsilon)+\hat{a}\cdot\vec{f}_1(\epsilon)$, while antiparallel to the field it is $f_0(\epsilon)-\hat{a}\cdot\vec{f}_1(\epsilon)$. The dimensional expression for $\hat{a}\cdot\vec{f}_1(\epsilon)$ is (see eq. (36)):

$$\hat{a}\cdot\vec{f}_1(\epsilon) = -\frac{n}{v_{th}^3}\frac{2}{qZ}\mathcal{E}\left[\frac{\epsilon^2}{1+\Omega^2\epsilon^3/(Z^2q^3)}\right]\frac{\partial f_0}{\partial\epsilon}. \tag{67}$$

Thus, for small magnetic fields, $f_1 \propto \epsilon^2\partial f_0/\partial\epsilon$, and the distribution function becomes more directional at higher energy (the runaway effect), but for large magnetic fields, $f_1 \propto \Omega^{-2}\epsilon^{-1}\partial f_0/\partial\epsilon$, and the distribution function becomes *less* directional at higher energy. The anisotropic collision-dominated low-energy behavior changes to the isotropic magnetic-dominated high-energy behavior at the maximum of $\hat{a}\cdot\vec{f}_1(\epsilon)/f_{MB}(\epsilon)$, which for a Maxwellian $f_0(\epsilon)$ is given by

$$\epsilon_{max} = q\left[\frac{2Z^2}{\Omega^2}\right]^{1/3} \tag{68}$$

Practically, of course, the magnetic field confines particles only within their cyclotron radius r_c; whether any real magnetic field-induced isotropy is obtained, or if instead a significant loss of particles occurs, is determined by the dimensions of the system. In a

finite-size system, the mean free path

$$\bar{\rho}(v_{th}) = \frac{v_{th}}{\nu_R + \bar{\nu}^*} \tag{69}$$

is an important quantity. (In this equation, $\bar{\nu}^*$ denotes the mean inelastic collision frequency). When an electron's mean free path exceeds the dimensions of the system, the electron can be said to have "run away", and the distribution function can be cut off at that energy. To estimate the number of electrons whose free path exceeds the given distance ρ, eq. (16) can be generalized, to give a "runaway" electron density of

$$n_\rho = 4\pi \int_{\epsilon(\rho)}^{\infty} d\epsilon \sqrt{\epsilon}\, f_0(\epsilon) \tag{70}$$

where $\epsilon(\rho)$ comes from inverting eq. (69); if only electron-electron collisions are considered, then

$$\epsilon(\rho) = q\sqrt{\rho/\bar{\rho}}. \tag{71}$$

Once an energy is somehow chosen at which electrons are deemed to be lost from the system by runaway, the rate at which electrons become runaways can be estimated by calculating the flux of electrons through a suitable surface in velocity space.[11,12] This flux is caused both by collisional diffusion and by the overall heating of the system. The runaway rate through a sphere in velocity space with radius corresponding to energy ϵ is

$$\Gamma(\epsilon) = -\frac{1}{n(\epsilon)} \frac{dn(\epsilon)}{dt} \tag{72}$$

where

$$n(\epsilon) = N(\epsilon) = 4\pi \int_0^{\epsilon} d\epsilon' \sqrt{\epsilon'}\, f_0(\epsilon'). \tag{73}$$

Note that the total density $n \equiv n(\infty) = 1$ in the normalized units adopted here. The runaway rate can be found by integrating from eq. (57), with $N(0) = D(0) = \zeta(0) = 0$:

$$\Gamma(\epsilon) = -\frac{4\pi}{N(\epsilon)} \left\{ \left[N(\epsilon) + \frac{2\tau_R}{3\tau} \frac{\partial \tau V}{\partial \tau} \epsilon^{3/2} \right] f_0(\epsilon) + \left[D(\epsilon) + \alpha\zeta(\epsilon) \right] \frac{\partial f_0(\epsilon)}{\partial \epsilon} \right.$$
$$\left. + \int_{max(\epsilon,\epsilon_j)}^{\epsilon+\epsilon_j} d\epsilon' \sqrt{\epsilon'}\, \nu^*(\epsilon') f_0(\epsilon') \right\} \tag{74}$$

For a Maxwellian distribution the Fokker-Planck terms $N(\epsilon)f_0(\epsilon)$ and $D(\epsilon)f_0{}'(\epsilon)$ in this expression cancel, and electron diffusion in velocity space is due only to compressional, ohmic and inelastic collision processes.

Self-Similar Solutions

The "standard" Fokker-Planck equation (which includes C'_{FP} only) causes the electrons to approach a Maxwell-Boltzmann distribution from any initial state. Those Fokker-Planck terms are present in the description given here; acting against the tendency to approach a Maxwellian, however, are the two new terms: the heating term represented by $\alpha\zeta(\epsilon)$, and the radiative cooling term represented by $C^*(\epsilon)$.

The ohmic heating term (eqs. (54)) can be written as

$$C_a(\epsilon) = AZq^{3/2}g(\epsilon) \tag{75}$$

where A is proportional to ω^{-2}, and the shape function

$$g(\epsilon) = \frac{\epsilon^3}{Z^2q^3/\Omega^2 + \epsilon^3} \tag{76}$$

determines where the heating is focused. A plot of $g(\epsilon)$ and its derivative is given in fig. (3). The function starts at zero, rises abruptly, and then asymptotically approaches its maximum value of 1 at high energies. Low-energy particles experience little heating, because the large low-energy collision rates effectively randomize the electron motion and prevent the electric field from doing net work. High-energy particles are easier to heat up because more phase space is available to them (this is reflected in the factor of v^2 in eq. (37)).

Ohmic heating is focused at the inflection point of $g(\epsilon)$, located at ϵ_{max} (see eq. (68)), at the transition point between the collisional and magnetized regions of the plasma. For "strong" magnetic fields ($\Omega/Z > 2$), $g(1) \approx 1$, the function $g(\epsilon)$ is roughly constant over most of the distribution, and most of the ohmic heating occurs below the thermal energy. For weak fields, on the other hand, the heating varies greatly over the distribution and is strongest in the tail. Both strong and weak field heating can occur in a z-pinch: the approximate magnitude of Ω is

$$\Omega \approx \frac{B}{1\text{ kG}}\left(\frac{kT}{100\text{ eV}}\right)^{3/2}\left(\frac{10^{18}\text{ cm}^{-3}}{n_e}\right) \tag{77}$$

When high-magnetic-field ohmic heating dominates and $g(\epsilon)$ is effectively constant, the distribution function has a self-similar form analogous to that which has been found

for laser-heated plasmas.[6] [See Appendix III for a derivation of the laser-heating inverse bremsstrahlung term.] When inelastic collisions are ignored, the self-similar form is[6,7]

$$f_{SS}(\epsilon,t) = \frac{a}{y(t)^{3/2}} e^{(-\epsilon/y(t))^{m/2}} \tag{78}$$

where m is determined by the relative strengths of the heating and elastic collision terms, and the normalization and kinetic energy integrals determine

$$a = \frac{m}{8\pi\Gamma(3/m)} \tag{79}$$

$$y = qkT\frac{\Gamma(3/m)}{\Gamma(5/m)} \tag{80}$$

The function f_{SS} is an exact solution to eq. (57) with no inelastic or compressional terms ($C^* = \vec{\nabla}\cdot\vec{V} = 0$), in two special cases: When elastic collision dominate ($\alpha = 0$), the solution is a Maxwell-Boltzmann distribution, which is just f_{SS} with $m = 2$ and y independent of time; and when ohmic heating dominates ($\alpha \rightarrow \infty$), the solution is f_{SS} with $m = 5$. In other cases, f_{SS} is an approximate solution to eq. (57).

When only ohmic heating influences the distribution ($\alpha \rightarrow \infty$), it is possible to analytically determine the value of m and $y(t)$ by substituting eq. (78) into eq. (57). The result is:

$$\frac{dy}{d\tau} = \frac{A_1 m}{2y\sqrt{\epsilon}} \left(\frac{\epsilon}{y}\right)^{m/2-2} \left[\frac{m-2-m(\epsilon/y)^{m/2}}{3-m(\epsilon/y)^{m/2}}\right] \tag{81}$$

where

$$A_1 = \alpha\zeta(\infty) = \frac{4q^{5/2}}{3\Omega^2}\alpha \tag{82}$$

This has a self-consistent (i.e., ϵ-independent) solution only for $m = 5$:

$$y(t) = \left(\frac{25}{4}At\right)^{2/5} + \text{const.} \tag{83}$$

An analytic solution for m and $y(t)$ is no longer possible when α is finite, since the elastic collision terms make the equation nonlinear and the inelastic collision terms are non-local. However, in the limit $\alpha \rightarrow 0$, the $m = 2$ Maxwell-Boltzmann solution must be recovered. Numerical solutions have given a reasonably accurate formula for the exponent m in the absence of inelastic scattering:[7]

$$m(\alpha) = 2 + \frac{3}{1 + 1.66/\alpha^{0.724}} \tag{84}$$

This is plotted as a function of the electric field (in V/cm) in fig. (4).

The time dependence of the kinetic energy of a self-similar solution can be found from the ohmic heating, compressional and inelastic collision terms alone, since the Fokker-Planck terms conserve energy:

$$\frac{d\langle E\rangle}{d\tau} = -4\pi\alpha \int_0^\infty \zeta(\epsilon)\frac{\partial f}{\partial \epsilon}\, d\epsilon - \frac{2\tau_R}{3}\vec{\nabla}\cdot\vec{V}\langle E\rangle + 4\pi \int_0^\infty \epsilon^{3/2} C^*(\epsilon)\, d\epsilon$$

$$= 4\pi A_1 \frac{a}{y^{3/2}} - \frac{2\tau_R}{3}\left(\vec{\nabla}\cdot\vec{V}\right) y \frac{\Gamma(5/m)}{\Gamma(3/m} - 4\pi \sum_{a\ states} \epsilon_{ab} \int_0^\infty \nu_{ab}(\epsilon) f(\epsilon)\sqrt{\epsilon}\, d\epsilon. \quad (85)$$

where the step function in C^* allows the lower limit of the integral to be zero.

It is an interesting fact that the self-similar distribution is left unchanged by compressional heating or cooling. This may be readily verified by substituting eq. (78) into the density-conserving compressional term from eq. (57)

$$C_C = \frac{A_2}{\sqrt{\epsilon}}\frac{\partial}{\partial \epsilon}\left(\epsilon^{3/2} f(\epsilon)\right), \quad (86)$$

where $A_2 = [2\tau_R/3r]\partial(rV)/\partial r$. The time-development equation $\partial f/\partial\tau = C_C$ is then satisfied for any value of m. More generally, if $f(\epsilon)$ is of the form

$$f_a(\epsilon) = y^{-3/2} g(\epsilon/y) \quad (87)$$

where $g(x)$ is an arbitrary function of its argument, then the compressional term can be written

$$C_C = -Ay\frac{\partial f}{\partial y}. \quad (88)$$

Thus, $f_a(\epsilon)$ maintains the same form at all times, with only y varying in time according to $dy/d\tau = A_2 y$. The parameter $y(t)$ is linearly proportional to the temperature of these distributions, since

$$kT \equiv \frac{1}{q}\langle E\rangle$$

$$= y\frac{1}{q}\int_0^\infty dx\, x^{3/2} g(x), \quad (89)$$

and so the temperature changes under compression at the rate

$$\frac{dT}{d\tau} = A_2(\tau)T. \quad (90)$$

If the compression factor A_2 were independent of time, C_C would cause the temperature of the system to change exponentially. Generally, however, A_2 depends on time, and other factors also contribute to f_0 in general. If the compressional term is combined with the electric field heating terms (but not the Fokker-Planck or inelastic terms), an equation for $dy/d\tau$ follows which is very similar to eq. (81):

$$\left(\frac{1}{y}+A_2\right)\frac{dy}{d\tau}=\frac{A_1 m}{2\epsilon^{5/2}}\left(\frac{\epsilon}{y}\right)^{m/2}\left[\frac{m-2-m(\epsilon/y)^{m/2}}{3-m(\epsilon/y)^{m/2}}\right] \tag{91}$$

As before, this has self-consistent solutions only when $m = 5$, when $y(\tau)$ satisfies

$$\frac{dy}{d\tau}=\frac{5A_1}{2y^{3/2}}\left(1+A_2 y\right) \tag{92}$$

5. Numerical method of solution

The time-dependent Fokker-Planck equation, eq. (57), is numerically solved, using implicit finite-differencing. Implicit differencing was chosen for its stability, but the simpler forward-differencing expression is also used to obtain estimates of the change in f with a particular time step.

For the differencing procedure, energy (velocity) space is divided into a possibly non-uniform grid; the grid-point index is denoted by a subscript. The energy at grid point j is ϵ_j, and the grid spacing is given by $\Delta\epsilon_j \equiv \epsilon_j - \epsilon_{j-1}$. In addition, the time evolution is separated into discrete steps of duration $\Delta\tau$, with the value of a quantity at a given time step denoted by a superscript. Eq. (57) is in the following form:

$$\frac{df}{d\tau}=\frac{1}{\sqrt{\epsilon}}\frac{\partial}{\partial\epsilon}F(\epsilon)-G(\epsilon) \tag{93}$$

with $F(\epsilon)$ representing the elastic terms and $G(\epsilon)$ representing the inelastic terms. This is implicitly finite-differenced as

$$\frac{1}{\Delta\tau}(f_j^{n+1}-f_j^n)=\frac{1}{\sqrt{\epsilon_j}}\left\{\frac{F_{j+1/2}^{n+1/2}-F_{j-1/2}^{n+1/2}}{\Delta\epsilon_{j+1/2}}\right\}-G_j^{n+1/2} \tag{94}$$

with the half-gridpoint values defined as (for both space and time):

$$f^{n+1/2}=\frac{1}{2}\left[f^{n+1}+f^n\right]. \tag{95}$$

Eq. (94) is then written out, with all of the future-time quantities f^{n+1} on the left, and all the past-time quantities f^n on the right-hand side. The abbreviations $\mathcal{N} = N(\epsilon) + \frac{2}{3}\tau_R \epsilon^{3/2} \partial V/\partial r$ and $\mathcal{D} = D(\epsilon) + \alpha\zeta(\epsilon)$ are introduced for brevity. The inelastic collision frequencies are denoted $\nu^*_{i,j}$, where the first subscript denotes the scattering process and the second gives the energy grid-point index. Collecting common factors, the result is:

$$
\begin{aligned}
&- \frac{\Delta\tau}{4\Delta\epsilon_{j+\frac{1}{2}}\sqrt{\epsilon_j}}\left(\mathcal{N}^n_{j+\frac{1}{2}} + \frac{2}{\Delta\epsilon_{j+1}}\mathcal{D}^n_{j+\frac{1}{2}}\right) f^{n+1}_{j+1} \\
&+ \left(1 - \frac{\Delta\tau}{4\Delta\epsilon_{j+\frac{1}{2}}\sqrt{\epsilon_j}}\left[\mathcal{N}^n_{j+\frac{1}{2}} - \mathcal{N}^n_{j-\frac{1}{2}} - \frac{2}{\Delta\epsilon_{j+1}}\mathcal{D}^n_{j+\frac{1}{2}} - \frac{2}{\Delta\epsilon_j}\mathcal{D}^n_{j-\frac{1}{2}}\right]\right) f^{n+1}_j \\
&+ \frac{\Delta\tau}{4\Delta\epsilon_{j+\frac{1}{2}}\sqrt{\epsilon_j}}\left(\mathcal{N}^n_{j-\frac{1}{2}} - \frac{2}{\Delta\epsilon_{j+1}}\mathcal{D}^n_{j-\frac{1}{2}}\right) f^{n+1}_{j-1} + \frac{\Delta\tau}{2}\sum_i \left(\nu^*_{ij} f^{n+1}_j - \nu^*_{i,j+l_i} f^{n+1}_{j+l_i}\right) \\
&\qquad = \frac{\Delta\tau}{4\Delta\epsilon_{j+\frac{1}{2}}\sqrt{\epsilon_j}}\left(\mathcal{N}^n_{j+\frac{1}{2}} + \frac{2}{\Delta\epsilon_{j+1}}\mathcal{D}^n_{j+\frac{1}{2}}\right) f^n_{j+1} \\
&\qquad\quad + \left(1 + \frac{\Delta\tau}{4\Delta\epsilon_{j+\frac{1}{2}}\sqrt{\epsilon_j}}\left[\mathcal{N}^n_{j+\frac{1}{2}} - \mathcal{N}^n_{j-\frac{1}{2}} - \frac{2}{\Delta\epsilon_{j+1}}\mathcal{D}^n_{j+\frac{1}{2}} - \frac{2}{\Delta\epsilon_j}\mathcal{D}^n_{j-\frac{1}{2}}\right]\right) f^n_j \\
&\qquad\quad - \frac{\Delta\tau}{4\Delta\epsilon_{j+\frac{1}{2}}\sqrt{\epsilon_j}}\left[\mathcal{N}^n_{j-\frac{1}{2}} - \frac{2}{\Delta\epsilon_j}\mathcal{D}^n_{j-\frac{1}{2}}\right] f^n_{j-1} \\
&\qquad\quad - \frac{\Delta\tau}{2}\sum_i \left(\nu^*_{ij} f^n_j - \nu^*_{i,j+l_i} f^n_{i,j+l_i}\right)
\end{aligned}
\tag{96}
$$

This can be written in matrix form as

$$T^n_{jk} f^{n+1}_k = U^n_{jk} f^n_k \tag{97}$$

which has the formal solution

$$f^{n+1} = (T^n)^{-1} U^n f^n \tag{98}$$

and all of the difficulty in obtaining the solution lies in inverting the matrix T. If it were not for the inelastic collision sums, T would be a tridiagonal matrix, whose inverse can be rapidly computed. With this in mind, it is worthwhile to examine how important these collision terms are. It has been shown that the overall contribution of inelastic collision to the kinetic equation is small. If the distribution function does not change rapidly, the

linear collision sum can be taken as constant between time steps, and the advanced-time collision term on the left-hand side of eq. (96) can be moved to the right-hand side. In this case, a tridiagonal matrix equation is obtained, which may be written as follows:

$$C^n f_{j+1}^{n+1} + (1 - B^n) f_j^{n+1} + A^n f_{j-1}^{n+1} = D^n + f_j^n \tag{99}$$

with

$$A^n = \frac{\Delta\tau}{4\Delta\epsilon_{j+\frac{1}{2}}\sqrt{\epsilon_j}} \left(\mathcal{N}_{j-\frac{1}{2}}^n - \frac{2}{\Delta\epsilon_j} \mathcal{D}_{j-\frac{1}{2}}^n \right) \tag{100a}$$

$$B^n = \frac{\Delta\tau}{4\Delta\epsilon_{j+\frac{1}{2}}\sqrt{\epsilon_j}} \left(\mathcal{N}_{j+\frac{1}{2}}^n - \mathcal{N}_{j-\frac{1}{2}}^n - \frac{2}{\Delta\epsilon_{j+1}} \mathcal{D}_{j+\frac{1}{2}}^n - \frac{2}{\Delta\epsilon_j} \mathcal{D}_{j-\frac{1}{2}}^n \right) \tag{100b}$$

$$C^n = -\frac{\Delta\tau}{4\Delta\epsilon_{j+\frac{1}{2}}\sqrt{\epsilon_j}} \left(\mathcal{N}_{j+\frac{1}{2}}^n + \frac{2}{\Delta\epsilon_{j+1}} \mathcal{D}_{j+\frac{1}{2}}^n \right) \tag{100c}$$

$$D^n = -C^n f_{j+1}^n + B^n f_j^n - A^n f_{j-1}^n - \Delta\tau \sum_i \left(\nu_{ij}^* f_j^n - \nu_{i,j+l_i}^* f_{j+l_i}^n \right) \tag{100d}$$

While the implicit differencing scheme is a particularly stable method for the solution of eq. (57), a simple forward-differencing of the equation gives simpler results, from which an upper bound to the time step $\Delta\tau$ can be derived. For the forward-differencing of eq. (57), eq. (94) is replaced by:

$$\begin{aligned} f_j^{n+1} - f_j^n = \frac{\Delta\tau}{\Delta\epsilon_{j+\frac{1}{2}}\sqrt{\epsilon_j}} \Bigg[& \frac{1}{2} \mathcal{N}_{j+\frac{1}{2}}^n \left(f_{j+1}^n + f_j^n \right) + \frac{1}{\Delta\epsilon_{j+1}} \mathcal{D}_{j+\frac{1}{2}}^n \left(f_{j+1}^n - f_j^n \right) \\ & - \frac{1}{2} \mathcal{N}_{j-\frac{1}{2}}^n \left(f_j^n + f_{j-1}^n \right) - \frac{1}{\Delta\epsilon_j} \mathcal{D}_{j-\frac{1}{2}}^n \left(f_j^n - f_{j-1}^n \right) \Bigg] \\ & + (\Delta\tau) G_j^n \end{aligned} \tag{101}$$

The solution for the advanced-time distribution function (corresponding to eq. (99)), is:

$$f_j^{n+1} = f_j^n + 2D^n + (\Delta\tau) G_j^n \tag{102}$$

where D^n is defined in eq. (100d).

This estimate of f^{n+1} can be used to fix an upper bound to $\Delta\tau$ such that the change over one time step is relatively small. For this estimate, the small inelastic term G_j^n,

involving sums over the different present-time distribution function values f_j^n, is ignored. If the desired change is limited to δ:

$$\left|(f^{n+1} - f^n)/f^n\right| \leq \delta, \tag{103}$$

then $\Delta\tau$ must satify the following relation:

$$\Delta\tau \leq \left|\frac{\delta}{2}\frac{f^n}{(D^n/\Delta\tau)}\right| \tag{104}$$

where $D^n/\Delta\tau$ is independent of $\Delta\tau$. In the numerical computations, $(f^{n+1} - f^n)/f^n$ was limited to $\delta = 0.1$ by means of eq. (104).

The procedure followed in the calculations, then, is to: (1) set up the initial state by specifying f_j^0 on the grid; (2) limit the time step according to eq. (104); and (3) compute the tridiagonal elements A, B and C of the matrix T from the distribution. Next, (4) the matrix is inverted and (5) is used in eq. (98) to compute the distribution function at the next time step. These steps are repeated to follow the progress of the system in time.

Energy conservation and normalization

Since accurate computation of changes in the energy is important in the solution, it is particularly important to properly difference the nonlinear Fokker-Planck coefficients $N(\epsilon)$ and $D(\epsilon)$. It is readily verified that the Fokker-Planck equation without heating or cooling terms conserves energy; that is, the time derivative of the kinetic energy, as calculated by eq. (16), proves to be zero. If this calculation is performed, it will be seen that conservation follows from the following relation:

$$\frac{\partial D}{\partial \epsilon} = 4\pi\sqrt{\epsilon}\int_{\epsilon}^{\infty} d\epsilon' f(\epsilon'), \tag{105}$$

which follows from the definition of eq. (53). Using this formula rather than eq. (53) to calculate D ensures numerical energy conservation. This result was first reported by Kho[8]. With this relation it is simple to show that, for a Maxwellian distribution of the form $f(\epsilon) = A\epsilon^{-\epsilon/kT}$,

$$\frac{D(\epsilon)}{N(\epsilon)} = kT. \tag{106}$$

For $N(\epsilon)$, a straightforward differencing of eq. (52) is sufficient.

Since the energy of the dynamic system changes in time, a normalization of the energy coordinate which was based on the system energy might also change in time. This was certainly true of the density normalization, which changes in time because of the compressional term; the density variation, however, could be analytically evaluated and then incorporated into the compressional term (see eq. (44)). This cannot be done for the energy variation. Therefore, a time-invariant normalization was employed: the dimensionless velocity is obtained with the initial thermal velocity, not the time-varying one. At the start of the system evolution, the average normalized energy density $\langle E \rangle = q = 3/2$; at later times it varies freely. This means, for example, that a later-time Maxwellian has the form $f(\epsilon) = A \exp[-\epsilon(kT(0)/kT(t))]$. The initial thermal velocity is simply a convenient scaling factor, as are the other normalization constants employed; of course, they become less convenient the more the system changes from its initial state.

6. Numerical Results

Relaxation of an initially Gaussian electron distribution to a Maxwell-Boltzmann distribution is shown in fig. (5). (Note that in all plots of the distribution function, the quantity plotted is the ratio, $\gamma(\epsilon)$, of the actual distribution function with a Maxwellian distribution at the same temperature; thus, the equilibrium point in fig. (5) is a straight line at $\gamma(\epsilon) = 1$.) In this calculation, only the electron-electron collision terms were nonzero. The initial distribution was given by $f(\epsilon) = a_0 \exp(-10[(\xi - p)/w]^2)$, where ξ is the dimensionless velocity of eq. (38) and a_0, p and w are constants determining normalization, gaussian center position and width, respectively. For fig. (5), the values $p = 0.3$ and $w = 0.3$ have been taken. The result appears to agree with that of Kho[8] for the same parameters. It can be seen in the plot that the equilibration time at any energy is roughly proportional to the electron-electron collision time.

When there is ohmic heating, the shape of the evolving distribution depends on the strength of the magnetic field. Strong-magnetic-field ohmic heating results in a depressed tail, as is shown in the time-development plots for both weak heating (fig. (6), $m = 2.5$) and strong heating (fig. (7), $m = 4.0$). These distributions, evolving from an inital Maxwellian,

rapidly take on the self-similar shape for heating which was described above. (The ratio of the self-similar distribution, eq. (78), with a Maxwellian has a peak at an energy which is easily shown to be proportional to the temperature; the heating up of the distribution can be seen in the figures by the advance in the peak locaton.)

Weak-magnetic-field ohmic heating is centered at an electron energy ϵ_{max} (eq. (68)) which depends on $\Omega^{-2/3}$; the distribution is enhanced relative to the same-temperature Maxwellian in the vicinity of ϵ_{max}, and high-energy runaway production is possible. In fig. (8), the time-evolution of an initially Maxwellian distribution is shown for ohmic heating focused at $\epsilon = 5$ ($\Omega = 0.2324Z$). As long as the magnetic field is finite, the highest-energy electrons will always be confined, and the distribution tail must be depleted relative to a Maxwellian; for low enough fields, however, an enhancement can be seen over a significant fraction of the high-energy electron population.

Inelastic collisions cause a relative enhancement in the distribution function tail. This can be seen in fig. (9), which shows the evolution of a system under the sole influence of inelastic collisions. For simplicity, only one inelastic process was included, with a collision strength $\Omega_{ab} = 1$; the same behavior holds true in general. There is a depletion in the distribution function near the threshhold energy ϵ_{ab}, but everywhere else the distribution function is enhanced over the Maxwellian value. This is a surprising result, since the effect of inelastic collisions is to move electrons from higher to lower energy states. Collisions lower the temperature much more effectively than they reduce the high-energy electron population, however, and the enhanced tail of fig. (9) is the result.

The effect of compression is shown in fig. (10), where a non-Maxwellian distribution (obtained as in fig. (8) by ohmic heating) is compressed. The result is a more or less isomorphic heating of the distribution. Just as in fig. (6) and the following figures, the peak in the ratio $f_0(\epsilon)/f_{MB}$ moves to the right as the distribution is heated. As was shown here, if the initial distribution has the form of the self-similar solution (eq. (78)), including the Maxwellian, compressional heating is completely isomorphic: only the temperature is changed by compression (with appropriate shifts in the peak of the ratio with the Maxwellian).

These figures illustrate the individual effects of the various Fokker-Planck terms of the

electron distribution. In a z-pinch implosion, these terms are interacting and competing to produce a dynamically changing distribution function, which may at times be Maxwellian and at other times be strongly non-Maxwellian. The numerical code spelled out here can be used both to follow the changes of this distribution function and to estimate the effects of its variation. The determining factors are the external parameters of temperature, degree of ionization, mean velocity, and electric and magnetic fields. These parameters could obtained from a hydrodynamic model, for example, which solves for the spatial variation of a given system, and the calculated velocity distribution function could be used to estimate runaway production, radiation output, and the self-consistency of the hydrodynamic model. Results from this diagnostic use of the Fokker-Planck solution will be reported in subsequent works. A hybrid hydrodynamic-kinetic model could also be constructed, where the transport coefficients are calculated from the true distribution function instead of an assumed Maxwellian. This procedure could be both more accurate and more robust in analyzing the variety of possible z-pinch implosions.

Acknowledgements

The authors wish to thank N.R. Pereira for his interest and suggestions, and gratefully acknowledge the assistance of J. Ambrosiano in formulating the numerical solution to the Fokker-Planck equation.

This work was supported in part by the Defense Nuclear Agency and by the Office of Naval Research.

APPENDIX I

The Fokker-Planck Collision Term

Here, the Fokker-Planck collision term which is written out in eq. (20a) is derived. This derivation is not from "first principles"; it is mainly intended to enable comparison with other forms of the collision term found the literature. A more detailed treatment of the statistics-related Fokker-Planck equation can readily be found in the literature, along

with the application to Coulomb scattering employed here[4].

We consider the effect of collisions with one particle species on the distribution function of another species. Species a has mass m and distribution function $f(v)$, while species b has mass M and distribution function $F(v)$. Changes are computed which result from a particles (e.g., electrons), with velocity v, being incident on b particles (e.g., ions), with velocity v'. The relative velocity is $\vec{\vartheta} = \vec{v} - \vec{v}'$.

The "Landau form" of the Fokker-Planck collision term is

$$\left(\frac{\delta f_a}{\delta t}\right)_{ab} = Y_{ab}\vec{\nabla}\cdot\Gamma(v) \tag{I.1}$$

where

$$\Gamma = \frac{1}{2}\int d^3v' \left[\frac{\overleftrightarrow{I}\vartheta^2 - \vec{\vartheta}\vec{\vartheta}}{\vartheta^3}\right]\cdot\left[F(v')\vec{\nabla}_v f(v) - \frac{m}{M}f(v)\vec{\nabla}_{v'}F(v')\right], \tag{I.2}$$

and Y_{ab} is defined in eq. (21). The gradient operator $\vec{\nabla}$ acts on the variable $\vec{v}$ unless otherwise specified.

To rewrite eq. (I.1), it is useful to note that

$$\frac{\overleftrightarrow{I}\vartheta^2 - \vec{\vartheta}\vec{\vartheta}}{\vartheta^3} = \vec{\nabla}_v\vec{\nabla}_v\vartheta \tag{I.3}$$

By commuting the $\vec{\nabla}_v$ operations, integrating by parts with $\vec{\nabla}_{v'}$, and using $\vec{\nabla}_{v'} = -\vec{\nabla}_v$, it can easily be shown that

$$\left(\frac{\delta f}{\delta t}\right)_{ab} = -\vec{\nabla}\cdot\left[\vec{A}(\vec{v})f(\vec{v})\right] + \frac{1}{2}\vec{\nabla}\vec{\nabla}:\left[\overleftrightarrow{B}(\vec{v})f(\vec{v})\right] \tag{I.4}$$

where

$$\vec{A}(\vec{v}) = \frac{m+M}{M}Y_{ab}\vec{\nabla}\int d\vec{v}'\frac{F(\vec{v}')}{|\vec{v}-\vec{v}'|} \tag{I.5}$$

$$\overleftrightarrow{B} = Y_{ab}\vec{\nabla}\vec{\nabla}\int d\vec{v}'|\vec{v}-\vec{v}'|F(\vec{v}') \tag{I.6}$$

The quantity $\vec{A}(\vec{v})$ is called the coefficient of dynamic friction, and $\overleftrightarrow{B}(\vec{v})$ is called the diffusion coefficient. The integrals $\int dv'F(v')\vartheta$ and $\int dv'F(v')/\vartheta$ in the above expressions are called the Rosenbluth potentials.

The Cartesian tensor expansion of eq. (13) can now be employed in eq. (I.4) to obtain equations which are satisfied by each expansion term. A spherical coordinate system is used to evaluate the integrals. Of course, only a magnitude-of-v dependence will be left in the final expression, though the direction of $\vec{f}_1(v)$ will preserve (to first order) the directionality of the system. It is straightforward to calculate the equation for $f_0(v)$. Higher-order terms are more complicated, since these involve vector, tensor, etc. components, and the coefficients $\vec{A}(v)$ and $\overleftrightarrow{B}(v)$ must be expanded. This will not be done here (see Shkarofsky[4], section 7-5, for details).

Expressions are given below for the required derivatives in spherical coordinates, when there is only a $|\vec{v}|$ dependence (with unit basis vectors $\{\hat{e}_i\}$).

$$\vec{\nabla}\phi = \hat{e}_i \frac{v_i}{v}\frac{\partial \phi}{\partial v} \tag{I.7}$$

$$\vec{\nabla}\vec{\nabla}\phi = \hat{e}_i\hat{e}_j\left[\delta_{ij}\frac{1}{v}\frac{\partial\phi}{\partial v} + \frac{v_i v_j}{v^2}\left(\frac{\partial^2\phi}{\partial v^2} - \frac{1}{v}\frac{\partial\phi}{\partial v}\right)\right] \tag{I.8}$$

$$\equiv \hat{I}\varphi(v) + \hat{v}\hat{v}\psi(v) \tag{I.9}$$

$$\vec{\nabla}\vec{\nabla} : \vec{\nabla}\vec{\nabla}\phi = \vec{\nabla}\cdot\left[\vec{\nabla}\cdot\vec{\nabla}\vec{\nabla}\phi\right]$$

$$= \frac{\partial}{\partial v_i}\left\{\frac{v_i}{v}\left[\frac{\partial\varphi}{\partial v} + \frac{2}{v}\psi + \frac{\partial\psi}{\partial v}\right]\right\} \tag{I.10}$$

$$= \frac{2}{v}\frac{\partial\varphi}{\partial v} + \frac{\partial^2\varphi}{\partial v^2} + \frac{2}{v^2}\psi + \frac{4}{v}\frac{\partial\psi}{\partial v} + \frac{\partial^2\psi}{\partial v^2} \tag{I.11}$$

In evaluating $\vec{A}(v)$ and $\overleftrightarrow{B}(v)$, the following easily derived identities are useful:

$$\int_0^\pi d\theta\,\sin\theta\frac{1}{|\vec{v}-\vec{v}'|} = \frac{2}{\max(v,v')} \tag{I.12}$$

$$\int_0^\pi d\theta\,\sin\theta|\vec{v}-\vec{v}'| = \begin{cases} 2\left(v + \dfrac{v'^2}{3v}\right), & \text{if } v' < v; \\ 2\left(v' + \dfrac{v^2}{3v'}\right), & \text{if } v' > v. \end{cases} \tag{I.13}$$

Using these identities it is easy to show that

$$\int d\vec{v}'\,\frac{F_0(v)}{|\vec{v}-\vec{v}'|} = 4\pi\left\{\frac{1}{v}\int_0^v dv' v'^2 F_0(v') + \int_v^\infty dv' v' F_0(v')\right\} \tag{I.14}$$

$$\int d\vec{v}'|\vec{v}-\vec{v}'|F_0(v) = 4\pi\left\{v\int_0^v dv' v'^2 F_0(v') + \frac{1}{3v}\int_0^v dv' v'^4 F_0(v')\right.$$

$$\left. + \int_v^\infty dv' v'^3 F_0(v') + \frac{v^2}{3}\int_v^\infty dv' v' F_0(v')\right\} \tag{I.15}$$

and so

$$\vec{A}_0 = -\frac{8\pi Y_{ee}}{v^2}\,\hat{v}\int_0^v dv' v'^2 F_0(v') \tag{I.16}$$

$$\vec{\vec{B}}_0 = 4\pi Y_{ee}\left\{\hat{I}\left[\frac{1}{v}\int_0^v dv' v'^2 F_0(v') - \frac{1}{3v^3}\int_0^v dv' v'^4 F_0(v') + \frac{2}{3}\int_v^\infty dv' v' F_0(v')\right]\right.$$
$$\left. + \hat{v}\hat{v}\left[\frac{1}{v^3}\int_0^v dv' v'^4 f(v') - \frac{1}{v}\int_0^v dv' v'^2 f(v')\right]\right\} \tag{I.17}$$

These expressions can now be substituted into eq. (I.4), which to zeroth order is

$$\left(\frac{\delta f_0}{\delta t}\right)_c = \vec{\nabla}\cdot\left[-\vec{A}_0(v) f_0(v) + \frac{1}{2}\vec{\nabla}\cdot(\vec{\vec{B}}_0(v) f_0(v))\right] \tag{I.18}$$

$$= \frac{\partial}{\partial v_i}\left[\frac{v_i}{v}\frac{nY}{v^2}\left(N(v) f_0(v) + D(v)\frac{\partial f_0}{\partial v}\right)\right], \tag{I.19}$$

where the quantities $N(v)$ and $D(v)$ are defined as

$$N(v) = 4\pi\int_0^v dv'\, v'^2 F_0(v') \tag{I.20}$$

$$D(v) = \frac{4\pi}{3}\left[\frac{1}{v}\int_0^v dv'\, v'^4 F_0(v') + v^2\int_v^\infty dv'\, v' F_0(v')\right]. \tag{I.21}$$

Finally, since

$$\frac{\partial}{\partial v_i}\left[\frac{v_i}{v^3}X\right] = \frac{1}{v^2}\frac{\partial X}{\partial v}, \tag{I.22}$$

then the lowest-order expression for the Fokker-Planck collision term is

$$\left(\frac{\delta f_0}{\delta t}\right)_c = \frac{nY}{v^2}\frac{\partial}{\partial v}\left[N(v) f_0(v) + D(v)\frac{\partial f_0}{\partial v}\right]. \tag{I.23}$$

This is just eq. (20a).

APPENDIX II

Cartesian-Tensor Component Equations

In this section, component equations for the first two terms of the Cartesian tensor expansion of $f(\vec{r},\vec{v},t)$ are derived from eq. (7), the Boltzmann equation in stationary coordinates. These differ only slightly from eqs. (18), which were derived from eq. (12).

the Boltzmann equation in moving coordinates, and are identical if $V(r) = \text{const}$. Although the expansion relies on spherical symmetry, we will use Cartesian components in the development. The Boltzmann equation is

$$\frac{\partial f}{\partial t} + \vec{v} \cdot \vec{\nabla} f + (\vec{a} + \vec{v} \times \vec{\omega}) \cdot \vec{\nabla}_v f = C \tag{II.1}$$

The expansion used is

$$\begin{aligned} f(\vec{v}) &= f_0 + \frac{1}{v} \vec{v} \cdot \vec{f}_1 \\ &= f_0 + f_x \sin\theta \cos\phi + f_y \sin\theta \sin\phi + f_z \cos\theta \end{aligned} \tag{II.2}$$

The chain rule gives for $\vec{\nabla}_v$:

$$\vec{\nabla}_v = \sum_i \left\{ \frac{\partial v}{\partial v_i} \frac{\partial}{\partial v} + \frac{\partial \theta}{\partial v_i} \frac{\partial}{\partial \theta} + \frac{\partial \phi}{\partial v_i} \frac{\partial}{\partial \phi} \right\} \hat{e}_i \tag{II.3}$$

$$= \frac{\vec{v}}{v} \frac{\partial}{\partial v} + \frac{1}{v^2} \frac{\partial \vec{v}}{\partial \theta} \frac{\partial}{\partial \theta} + \frac{1}{v^2 \sin^2\theta} \frac{\partial \vec{v}}{\partial \phi} \frac{\partial}{\partial \phi} \tag{II.4}$$

When the expansion of eq. (II.2) is substituted into the Boltzmann equation, eq. (II.1), the various terms become:

$$\frac{\partial f}{\partial t} = \frac{\partial f_0}{\partial t} + \frac{\partial f_x}{\partial t} \sin\theta \cos\phi + \frac{\partial f_y}{\partial t} \sin\theta \sin\phi + \frac{\partial f_z}{\partial t} \cos\theta \tag{II.5}$$

$$\begin{aligned} \vec{v} \cdot \vec{\nabla} f = {} & v \left(\sin\theta \cos\phi, \sin\theta \sin\phi, \cos\theta\right) \cdot \vec{\nabla} f_0 \\ & + v \left(\sin\theta \cos\phi, \sin\theta \sin\phi, \cos\theta\right) \cdot \\ & \quad \left[\sin\theta \cos\phi \vec{\nabla} f_x + \sin\theta \sin\phi \vec{\nabla} f_y + \cos\theta \vec{\nabla} f_z\right] \end{aligned} \tag{II.6}$$

$$\begin{aligned} \vec{a} \cdot \vec{\nabla}_v f = {} & a_x \left\{ \sin\theta \cos\phi \left[\frac{\partial f_0}{\partial v} + \sin\theta \cos\phi \frac{\partial f_x}{\partial v} + \sin\theta \sin\phi \frac{\partial f_y}{\partial v} + \cos\theta \frac{\partial f_z}{\partial v} \right] \right. \\ & + \frac{1}{v} \cos\theta \cos\phi \left[f_x \cos\theta \cos\phi + f_y \cos\theta \sin\phi - f_z \sin\theta \right] \\ & \left. + \frac{1}{v} \sin\phi \left[f_x \sin\phi - f_y \cos\phi \right] \right\} \\ & + a_y \left\{ \sin\theta \sin\phi \left[\frac{\partial f_0}{\partial v} + \sin\theta \cos\phi \frac{\partial f_x}{\partial v} + \sin\theta \sin\phi \frac{\partial f_y}{\partial v} + \cos\theta \frac{\partial f_z}{\partial v} \right] \right. \\ & + \frac{1}{v} \cos\theta \sin\phi \left[f_x \cos\theta \cos\phi + f_y \cos\theta \sin\phi - f_z \sin\theta \right] \end{aligned}$$

$$+\frac{1}{v}\cos\phi\left[-f_x\sin\phi+f_y\cos\phi\right]\Bigg\}$$
$$+a_z\Bigg\{\cos\theta\left[\frac{\partial f_0}{\partial v}+\sin\theta\cos\phi\frac{\partial f_x}{\partial v}+\sin\theta\sin\phi\frac{\partial f_y}{\partial v}+\cos\theta\frac{\partial f_z}{\partial v}\right]$$
$$+\frac{1}{v}\sin\theta\left[-f_x\cos\theta\cos\phi-f_y\cos\theta\sin\phi+f_z\sin\theta\right]\Bigg\} \tag{II.7}$$

$$\vec{v}\times\vec{\omega}\cdot\vec{\nabla}_v f=-\omega\cdot\vec{v}\times\vec{\nabla}_v f$$
$$=\omega_x\left[-f_y\cos\theta+f_z\sin\theta\sin\phi\right]+\omega_y\left[f_x\cos\theta-f_z\sin\theta\cos\phi\right]$$
$$+\omega_z\left[\sin\theta(-f_x\sin\phi+f_y\cos\phi)\right] \tag{II.8}$$

To obtain an equation for f_0, the Boltzmann equation resuting from these substitutions is integrated over solid angle ($d^2\Omega=\sin\theta\,d\theta d\phi$). The results are

$$\int\frac{\partial f}{\partial t}\sin\theta\,d\theta d\phi=4\pi\frac{\partial f_0}{\partial t} \tag{II.9}$$
$$\int\vec{v}\cdot\vec{\nabla}f\sin\theta\,d\theta d\phi=\frac{4\pi}{3}v\vec{\nabla}\cdot\vec{f}_1 \tag{II.10}$$
$$\int\vec{a}\cdot\vec{\nabla}_v f\sin\theta\,d\theta d\phi=\frac{4\pi}{3}\frac{\partial}{\partial v}(\vec{a}\cdot\vec{f}_1)+\frac{8\pi}{3v}\vec{a}\cdot\vec{f}_1 \tag{II.11}$$

To obtain an equation for $\vec{f}_1$, the same procedure is followed, multiplying the equation in turn by $\sin\phi$, $\cos\phi$, and $\cos\theta$. After numerical constants are divided out, the resulting two equations are[4]

$$\frac{\partial f_0}{\partial t}+\frac{v}{3}\vec{\nabla}\cdot\vec{f}_1+\frac{1}{3v^2}\frac{\partial}{\partial v}\left[v^2\vec{a}\cdot\vec{f}_1\right]=C_{FP}+C^* \tag{II.12}$$
$$\frac{\partial\vec{f}_1}{\partial t}+v\vec{\nabla}f_0+\vec{a}\frac{\partial f_0}{\partial v}+\vec{\omega}\times\vec{f}_1=\vec{C}_1 \tag{II.13}$$

APPENDIX III

Electric field – Laser Heating equivalence to Ohmic Heating

While this study is primarily concerned with ohmic heating, there is a direct analogy with laser heating by inverse bremsstrahlung, which has been well studied in the literature.[6] In this appendix, the electric field heating term from laser heating is derived. It is

remarkable that, under certain conditions, this is identical in form to that for ohmic heating derived earlier.

The starting point for the derivation is eq. (33) for the electric field heating term in the Fokker-Planck equation, and eq. (34) for $\vec{f}_1$. With laser heating, time variations in $\vec{f}_1$ cannot be ignored; they are, however, periodic. We assume that any background magnetic field is negligible compared to the electric field of the laser light, so $\vec{\omega} = 0$ in eq. (19b). Particles are accelerated by the laser electric field, which has intensity $I = cE^2/4\pi$, wavelength λ, and oscillation frequency $\omega_L = 2\pi c/\lambda$. The maximum oscillation velocity of the particles is $\vec{v}_0$, which is related to the intensity and frequency by

$$I = \frac{m^2\omega_L^2 v_0^2 c}{4\pi e^2}. \tag{III.1}$$

If I is in W/cm^2, λ is in microns, and kT is in keV, then the ratio of the oscillation velocity to the thermal velocity (with $q = 3/2$) is $\frac{1}{2}mv_0^2/kT = 3.73595 \times 10^{-16} I\lambda^2/kT$. The laser acceleration is

$$\vec{a}(t) = \vec{v}_0\omega_L \cos\omega_L t. \tag{III.2}$$

Under these assumptions, eq. (34) for $\vec{f}_1$ becomes

$$\frac{d\vec{f}_1}{dt} + \nu_{ei}\vec{f}_1 = -\vec{a}(t)\frac{\partial f_0}{\partial v} \tag{III.3}$$

As with ohmic heating, it is assumed that $\vec{f}_1$ varies in time much more rapidly than f_0. But instead of looking for equilibrium solutions for $\vec{f}_1(v,t)$, eq. (III.3) is solved for the time-dependent $\vec{f}_1$, and this solution is averaged over a full period of the (rapid) laser oscillation. The solution to the homogeneous version of eq. (III.3) (i.e., $a(t) = 0$) is

$$\vec{f}_1(t) = \vec{A}e^{-\nu_{ei}t} \tag{III.4}$$

with $\vec{A}$ an arbitrary constant. The solution when $a(t) \neq 0$ can be expressed in the same form:

$$\vec{f}_1(t) = \vec{B}(t)e^{-\nu_{ei}t} \tag{III.5}$$

where

$$\vec{B}(t) = -\int_{t_0}^{t} \vec{a}(t')\frac{\partial f_0}{\partial v}e^{\nu_{ei}t'}\,dt'. \tag{III.6}$$

The lower limit of integration is determined by the boundary condition, which in this case is set by the requirement that $\lim_{t\to-\infty} \vec{f}_1(t) = 0$. To realize this, the acceleration $a(t)$ from eq. (III.2) is "adiabatically turned on" by multiplying it by a factor $\exp(\epsilon t)$, where ϵ is infinitesimal, for $t < 0$. When this $a(t)$ is used, and if $\partial f_0/\partial v$ is assumed to be independent of time (at least on the time scale of the $\vec{f}_1$ variations), the general solution for $\vec{f}_1(t)$ is

$$\vec{f}_1(t) = -\vec{v}_0 \frac{\omega_L}{\omega_L^2 + \nu_{ei}^2} \frac{\partial f_0}{\partial v} (\nu_{ei} \cos\omega_L t + \omega_L \sin\omega_L t). \tag{III.7}$$

For the calculation of f_0, the rapidly oscillating values of $\vec{f}_1$ are averaged. This is accomplished as follows:

$$\left\langle \vec{a} \cdot \vec{f}_1 \right\rangle_t = \frac{\omega_L}{2\pi} \int_{\omega_L t=0}^{\omega_L t=2\pi} \vec{a}(t) \cdot \vec{f}_1(t)\, dt$$

$$= -\frac{\nu_{ei} v_0^2/2}{1 + (\nu_{ei}/\omega_L)^2} \frac{\partial f_0}{\partial v} \tag{III.8}$$

If this expression is used for $\vec{a} \cdot \vec{f}_1$, the laser heating term in eq. (33) is

$$C_a = C_L = \frac{n_i Y_{ei} v_0^2}{6v^2} \frac{\partial}{\partial v} \left[\frac{1}{v} \frac{1}{1 + (\nu_{ei}/\omega_L)^2} \frac{\partial f_0}{\partial v} \right] \tag{III.9}$$

When expressed in terms of the dimensionless-energy representation of eq. (57) ($\Omega_L = \omega_L/\nu_R$), the connection with the ohmic heating term can be clearly seen:

$$C_L = \frac{\alpha}{\sqrt{\epsilon}} \frac{\partial \zeta(\epsilon)}{\partial \epsilon}, \tag{III.10}$$

where

$$\alpha_L = Z \frac{v_0^2}{v_{th}^2} = \frac{2\pi Z}{q} \frac{r_e c}{\omega_L^2 kT} I \tag{III.11a}$$

$$\zeta_L(\epsilon) = \frac{2\Omega_L^2}{3Z^2\sqrt{q}} \frac{\epsilon^3}{1 + \Omega_L^2 \epsilon^3 / Z^2 q^3} \tag{III.11b}$$

The results for ohmic heating and for laser heating are thus equivalent, with an effective laser-heating "magnetic field"

$$\Omega_L = \Omega_{EB} \tag{III.12}$$

and an effective laser "electric field"

$$\mathcal{E}_L = \frac{\Omega_L}{\sqrt{2}} \frac{v_0}{v_{th}}$$
$$= \frac{\omega_p}{2\nu_R} \sqrt{\frac{I}{c[nmv_{th}^2/2]}}, \qquad \text{(III.13)}$$

where $nmv_{th}^2/2$ is the thermal energy density in the plasma.

APPENDIX IV

Numbers and Units

From the 1986-87 CRC Handbook:

$c = 2.99792458 \times 10^{10}$ cm/sec

$m = 9.109534 \times 10^{-28}$ g

$e = 1.6021892 \times 10^{-19}$ C $= 4.8032423 \times 10^{-10}$ statcoul

$\hbar = 1.0545887 \times 10^{-27}$ erg-sec

$Ry = 13.605826$ eV

$r_e = 2.8179380 \times 10^{-13}$ cm

$m_e c^2 = 5.1100258 \times 10^5$ eV $= 8.1872281 \times 10^{-7}$ erg

With these values, and with kT measured in eV and n_e in cm^{-3}, the following numeric formulas can be given:

$$\log \Lambda = 23.463306 + \log \left[\frac{(kT)^{3/2}}{\sqrt{n_e}} \right] \qquad \text{(IV.1)}$$

$$\nu_R = 2.1030335 \times 10^{-6} \frac{n_e}{(kT)^{3/2}} \log \Lambda \text{ sec}^{-1} \qquad \text{(IV.2)}$$

$$\omega_p = 5.641458 \times 10^4 \sqrt{n_e} \qquad \text{(IV.3)}$$

$$E_D = 9.7148016 \times 10^3 (\epsilon/c) \nu_P \sqrt{3kT} \text{ statvolt/cm}$$
$$= 8.0877853 \times 10^{-16} \nu_R \sqrt{kT} \text{ statvolt/cm} \qquad \text{(IV.4)}$$

$$B_D = 5.685680 \times 10^{-8} \nu_R \text{ Gauss} \qquad \text{(IV.5)}$$

REFERENCES

1. N.R. Pereira and J. Davis, *J. Appl. Phys.* 64:R1 (1988).
2. N.R. Pereira and K.G. Whitney, *Phys. Rev.* A38:319 (1988).
3. R.S. Cohen, L. Spitzer and P.M. Routly, *Phys. Rev.* 80:230 (1950).
4. I.P. Shkarofsky, T.W. Johnston and M.P. Bachynski, *The Particle Kinetics of Plasmas*, Addison-Wesley, 1966.
5. I.P. Shkarofsky, *Can. J. Phys.* 41:1753(1963), eq. (40).
6. B. Langdon, *Phys. Rev. Lett.* 44:575 (1980).
7. P. Alaterre, J.-P. Matte and M. Lamoureux, *Phys. Rev.* A34:1578 (1986).
8. T.H. Kho, *Phys. Rev.* A32:32 (1985).
9. C. Kittel, *Introduction to Solid State Physics* (sixth edition), John Wiley & Sons, 1986. See chapter 6, eq. (64).
10. H. Dreicer, *Phys. Rev.* 115:23 (1959), *Phys. Rev.* 117:329 (1960).
11. R.M. Kulsrud, Y-C. Sun, N.K. Winsor and H.A. Fallon, *Phys. Rev. Lett.* 31:690 (1973).
12. This approach was also used by Dreicer[10]; his calculated "runaway rate" is the rate of decay of f_0 due to the electron flux through a velocity-space sphere at radius $V_b = \sqrt{3E_D/qE}$. Dreicer used the Langevin equation to show that V_b was the boundary of the runaway region.

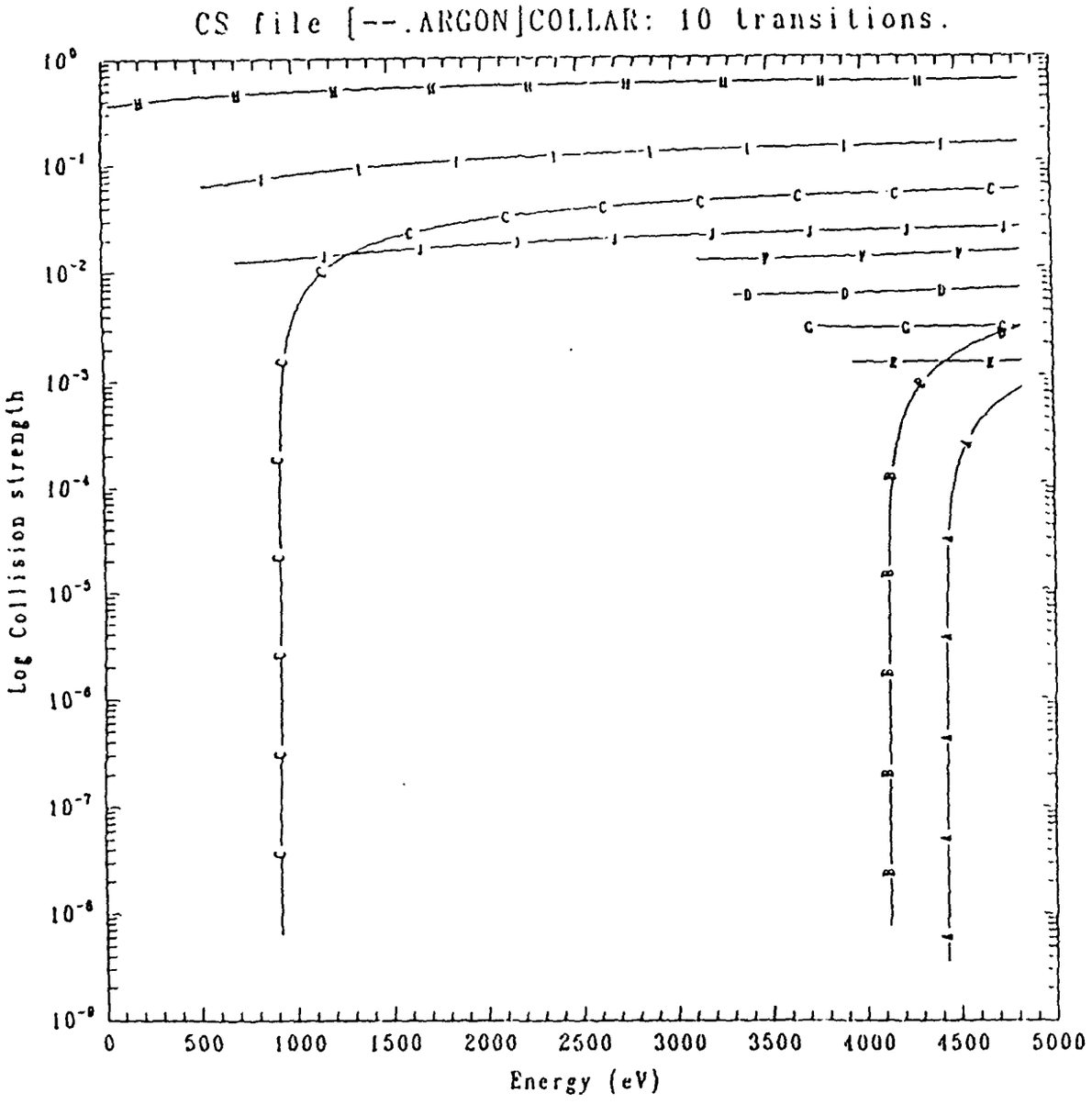

Figure 1. Some collision strengths for Argon. Each curve corresponds to a different inelastic process, with a threshold energy where the curve appears.

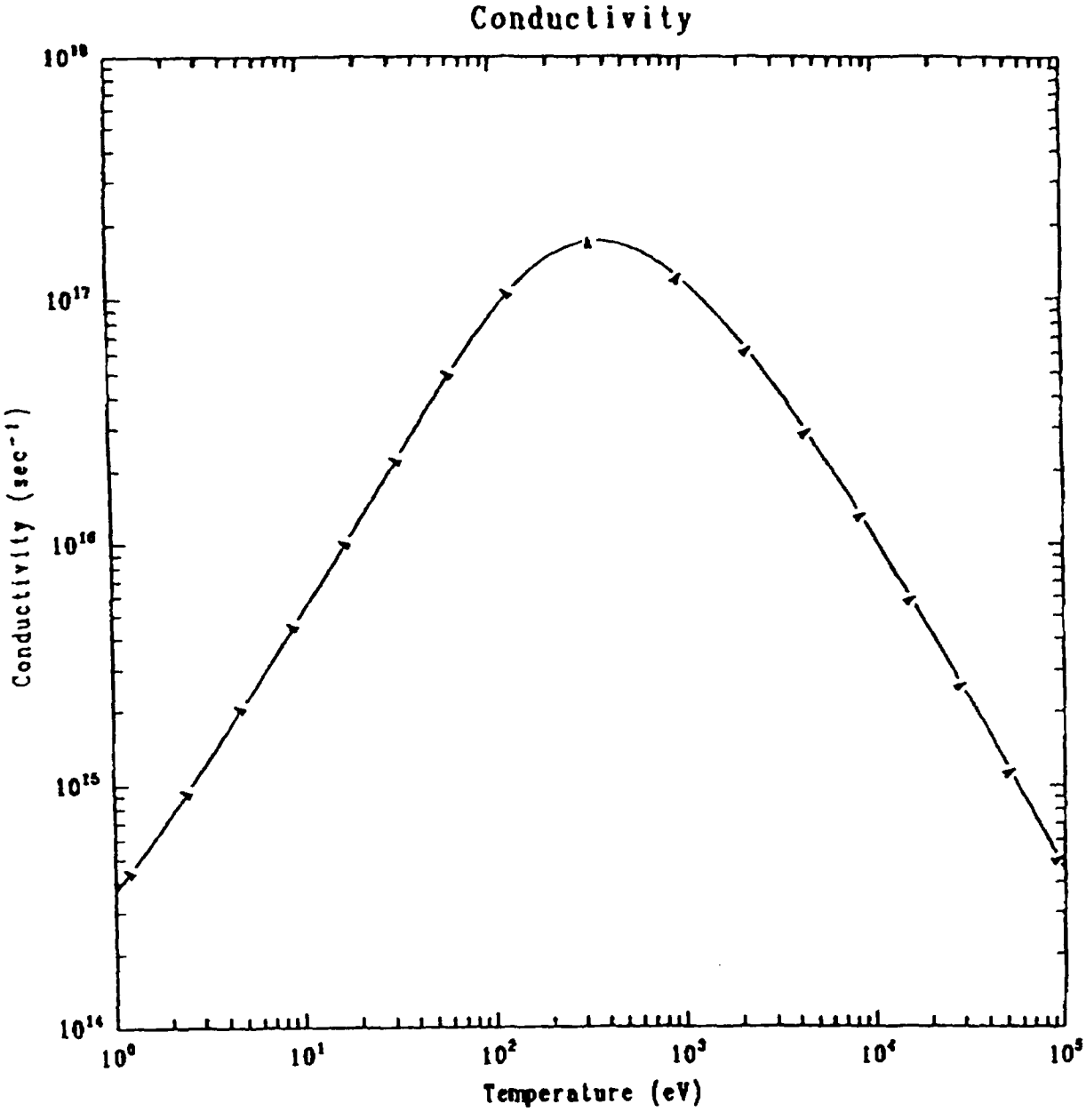

Figure 2. *Electron conductivity as a function of temperature. Suitable parameters have been chosen to exhibit the interaction between collisional resistance and magnetic confinement:* $Z = 1$, $B = 100\ G$, $n = 10^{18}\ cm^{-3}$.

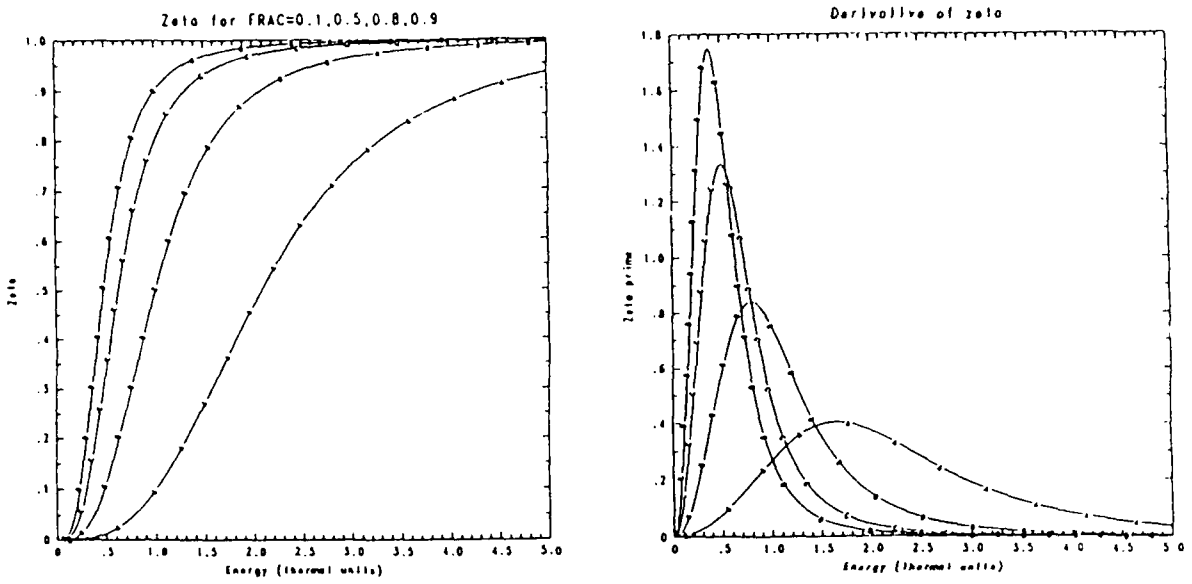

Figure 3. *The heating function $g(\epsilon)$ and its derivative as a function of ϵ for various values of the factor Z^2q^3/Ω^2 in the denominator (see eq. (76)).*

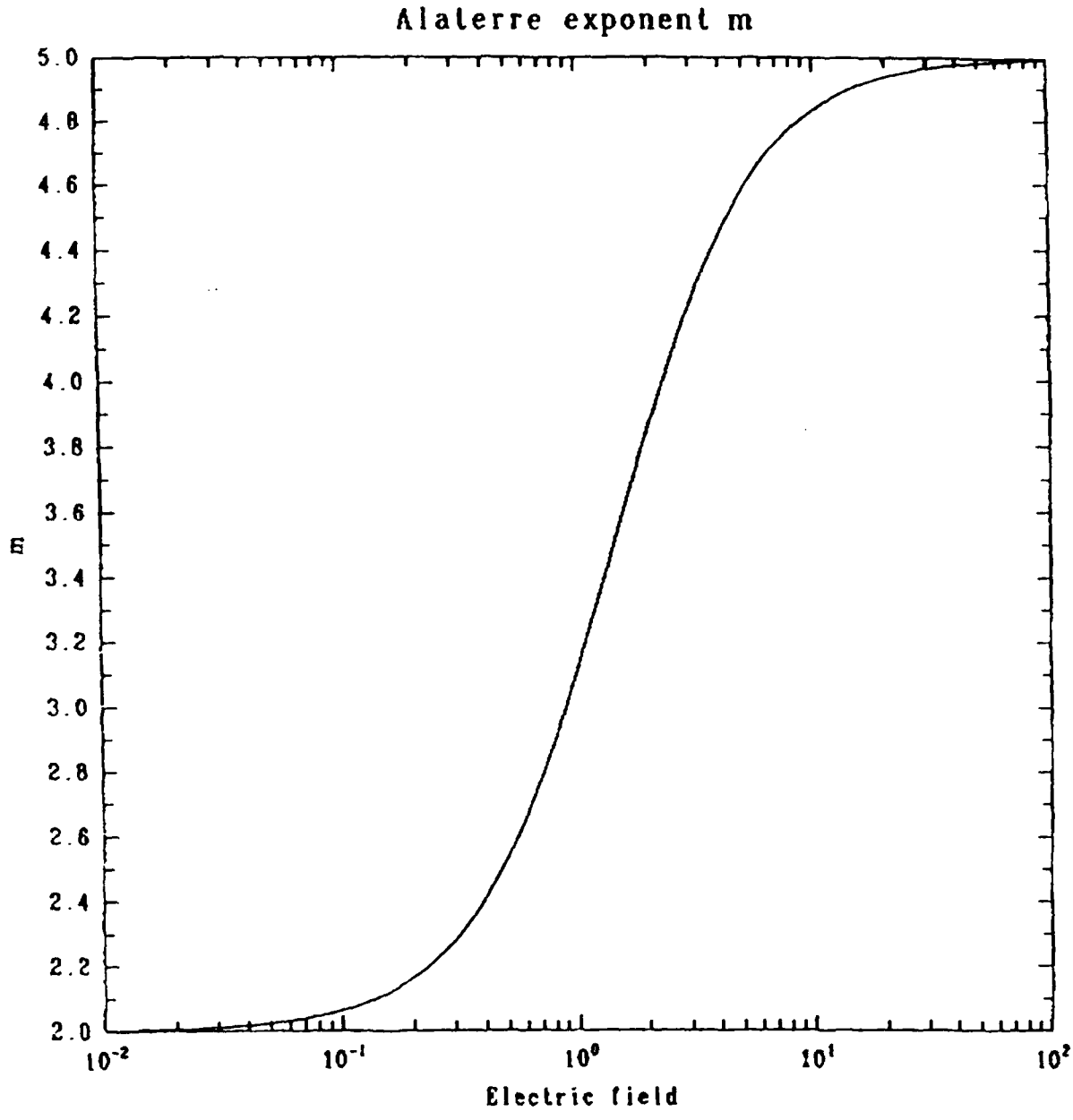

Figure 4. *Exponent m in the self-similar solution for the distribution function under high-magnetic-field heating, as a function of the electric field in units of E_D, the Dreicer field.*

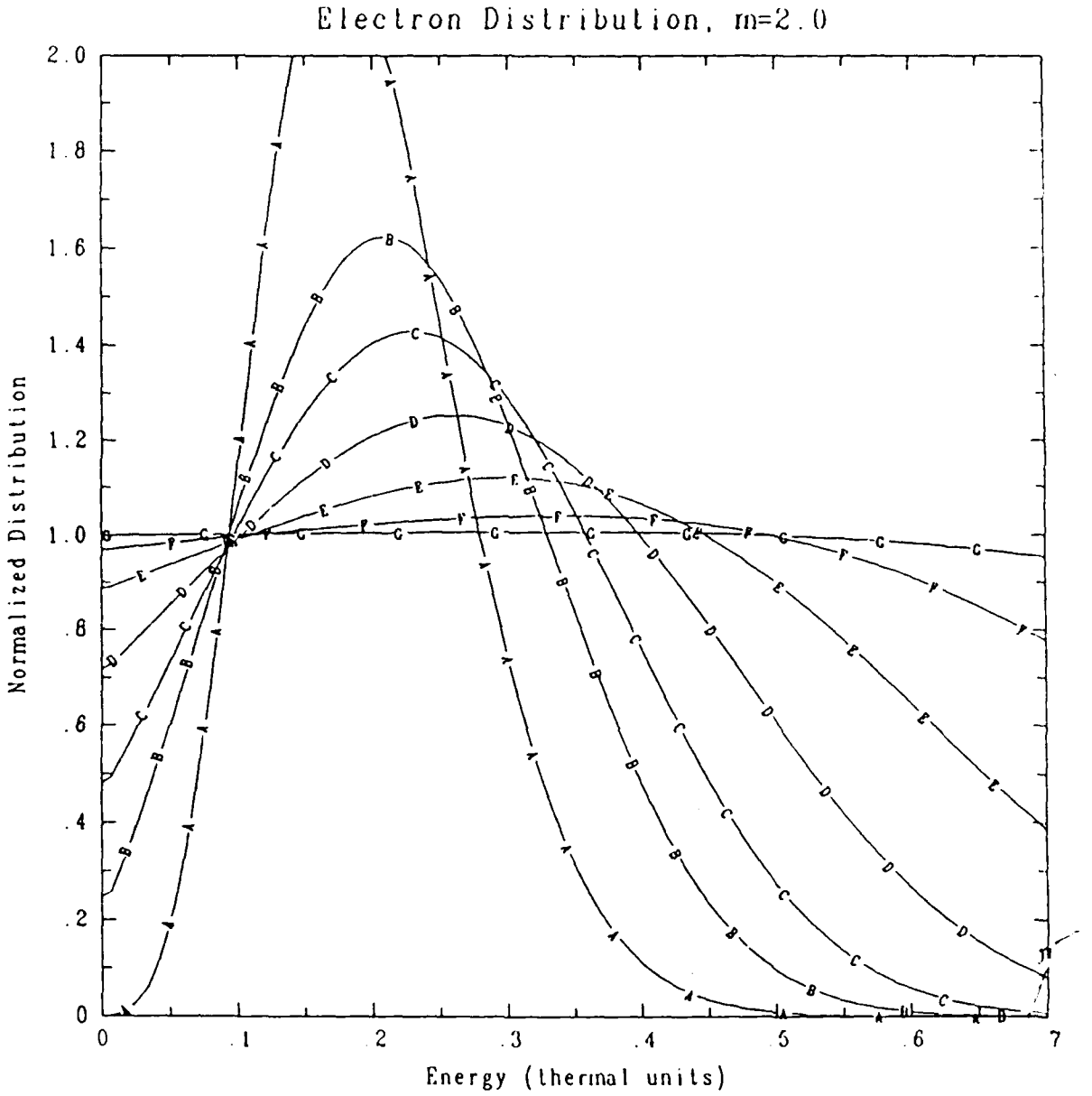

Figure 5. *Time-evolution of the distribution function from an initial Gaussian shape* $f(\epsilon) = a_0 e^{-10[(\epsilon-0.3)/0.3]^2}$ *to the equilibrium Maxwellian. Shown is the ratio* $f(\epsilon)/f_{MB}(\epsilon)$ *of the actual distribution with a Maxwellian at the same temperature. The various curves correspond to the times: A) initial condition; B) 0.02; C) 0.04; D) 0.08; E) 0.16; F) 0.32; and G) 0.64, in units of the thermal electron collision time* τ_R.

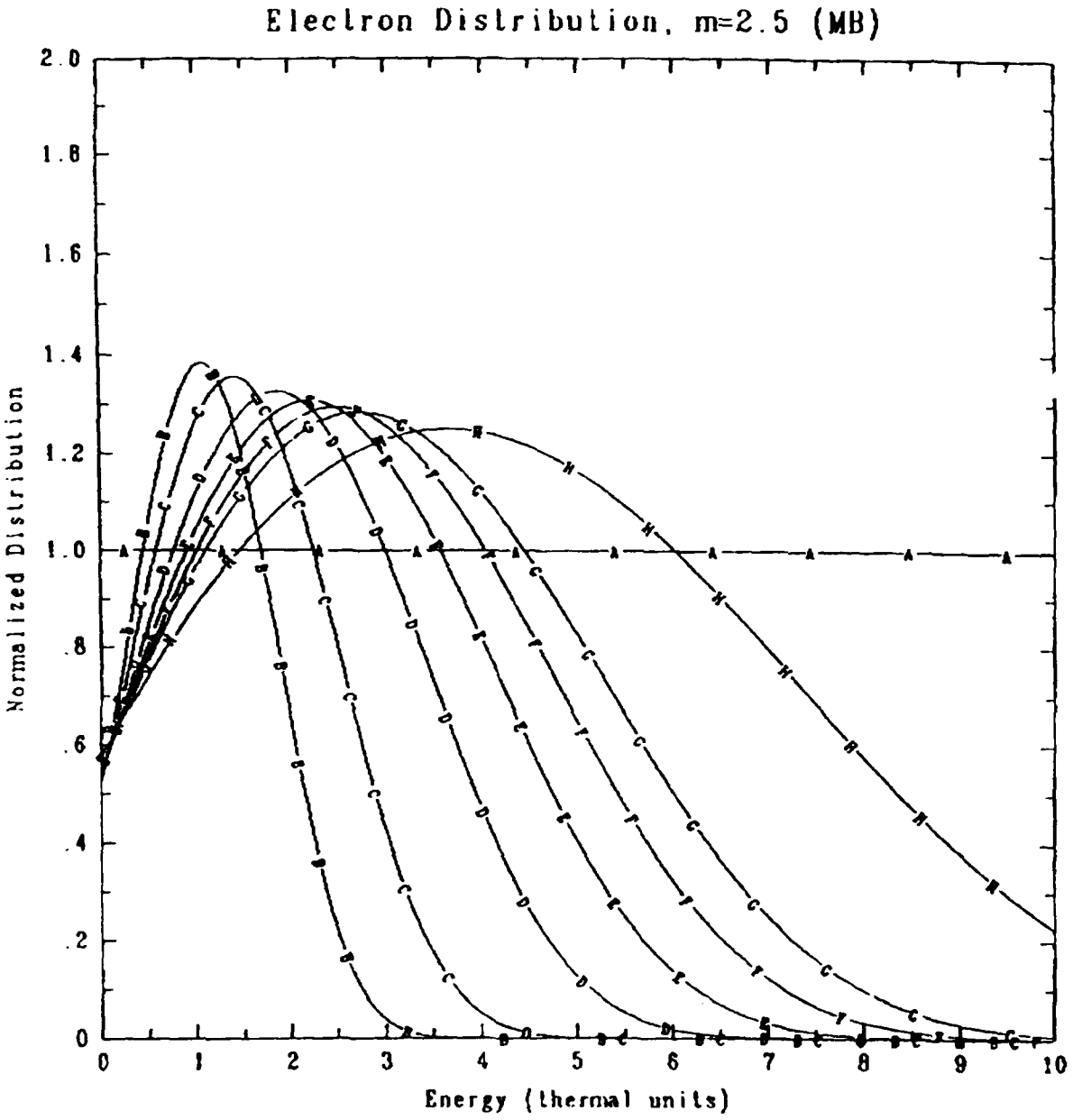

Figure 6. *Time-evolution of the distribution function from an initial Maxwellian, under the influence of strong-magnetic-field ohmic heating. The electric field is such that the exponent* $m = 2.5$. *Shown is the ratio* $f(\epsilon)/f_{MB}(\epsilon)$ *of the actual distribution with a Maxwellian at the same temperature, at times A) initial condition; B) 0.50; C) 1.00; D) 2.01; E) 3.01; F) 4.02; G) 5.01; and H) 10.06, in units of the thermal electron collision time* τ_R.

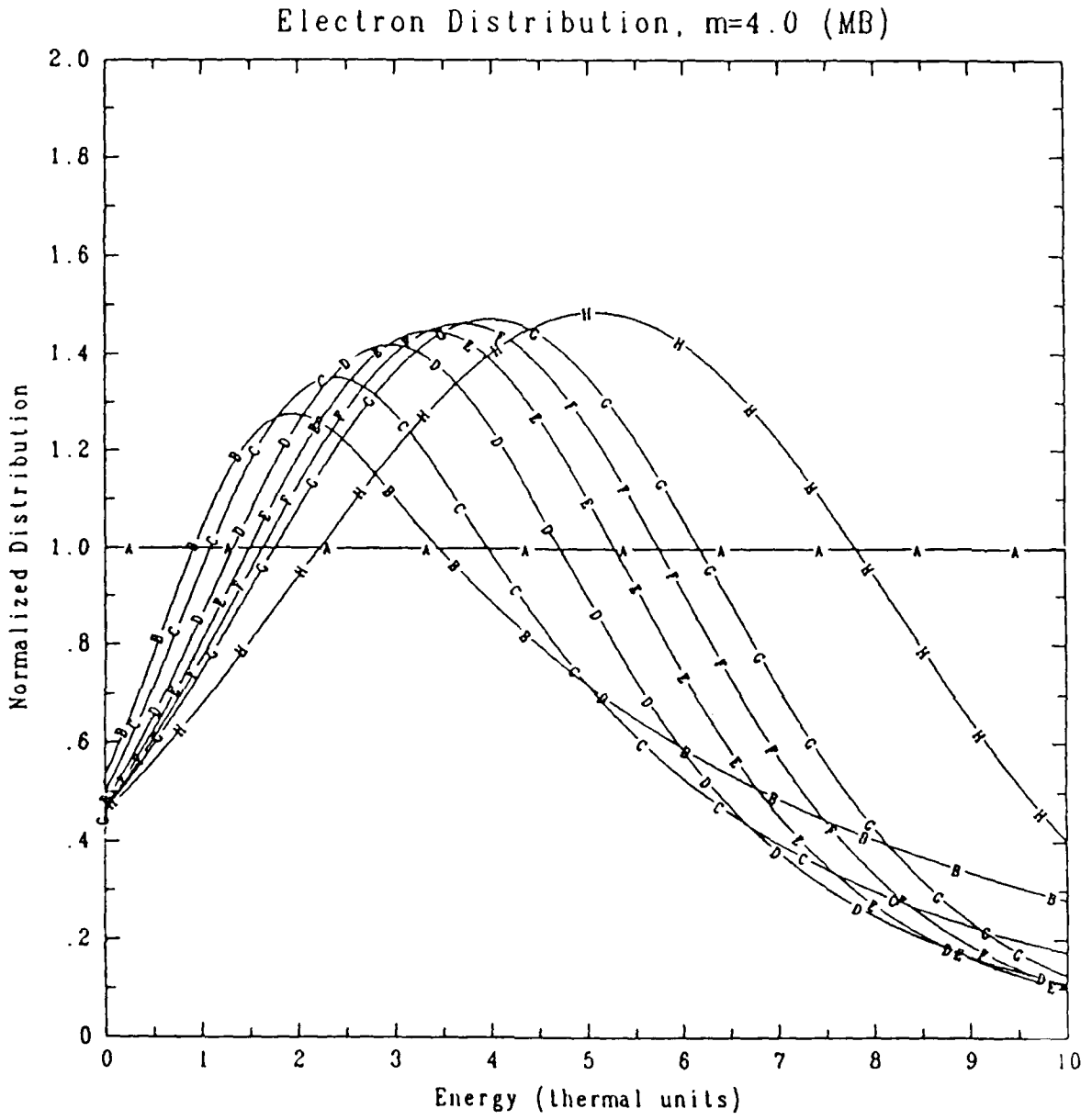

Figure 7. *Time-evolution of the distribution function from an initial Maxwellian, under the influence of strong-magnetic-field ohmic heating. The electric field is such that the exponent* $m = 4.0$. *Shown is the ratio* $f(\epsilon)/f_{MB}(\epsilon)$ *of the actual distribution with a Maxwellian at the same temperature, at times A) initial condition; B) 0.06; C) 0.11; D) 0.21; E) 0.31; F) 0.40; G) 0.50; and H) 1.00, in units of the thermal electron collision time* τ_R.

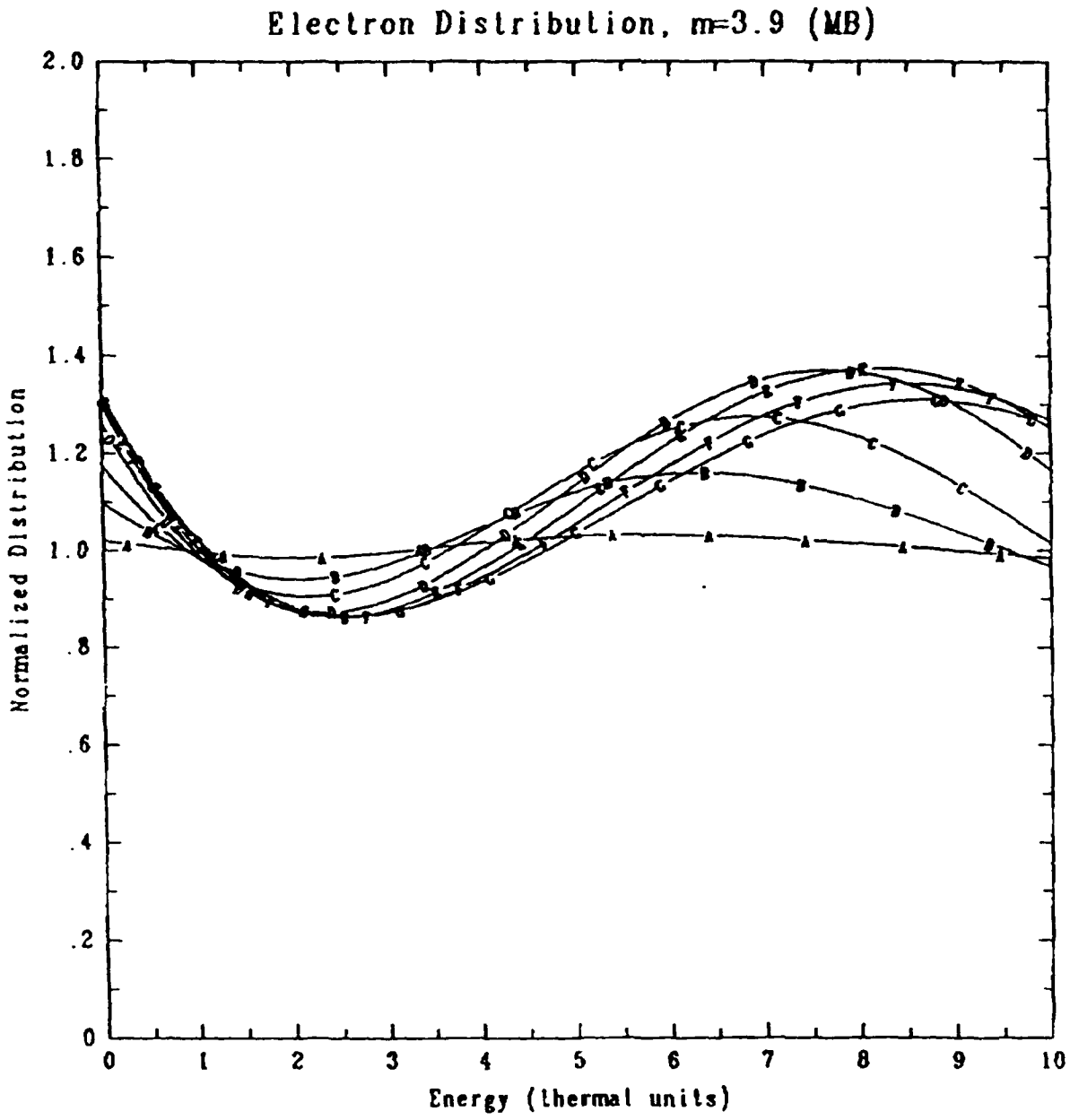

Figure 8. *Time-evolution of the distribution function from an initial Maxwellian, under the influence of weak-magnetic-field ohmic heating. Heating is focused at* $\epsilon = 5$. *The electric field is such that the exponent* $m = 2.5$. *Shown is the ratio* $f(\epsilon)/f_{MB}(\epsilon)$ *of the actual distribution with a Maxwellian at the same temperature, at times A) initial condition; B) 0.53; C) 1.08; D) 2.12; E) 3.15; F) 4.09; and G) 4.89, in units of the thermal electron collision time* τ_R.

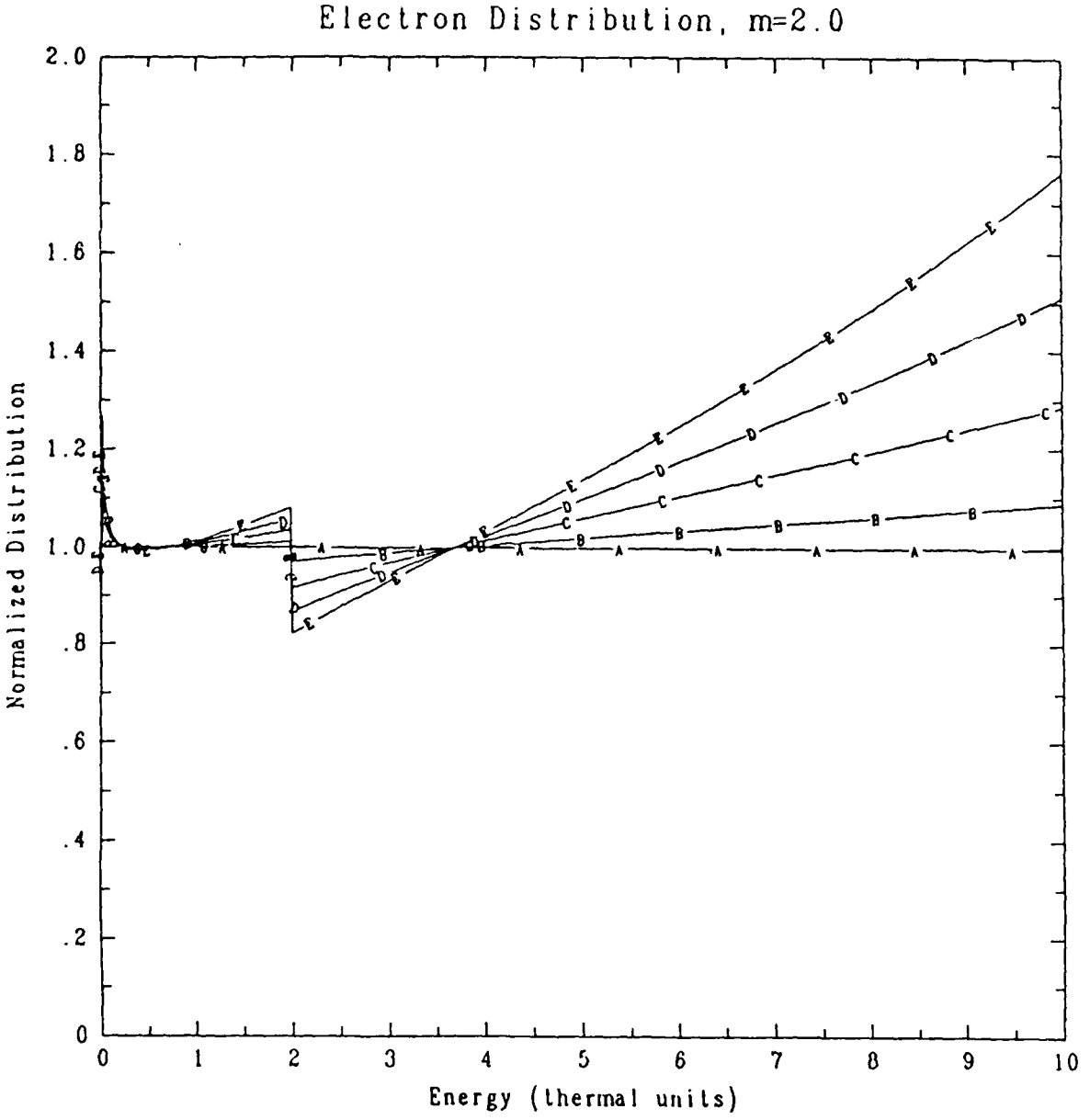

Figure 9. *Time-evolution of the distribution function from an initial Maxwellian under the influence of inelastic collisions only. Only one inelastic processes is present, with a threshold at $\epsilon = 2$. The collision strength has been set to $\Omega = 1000$, an unrealistically high value, for display purposes. Shown is the ratio $f(\epsilon)/f_{MB}(\epsilon)$ of the actual distribution with a Maxwellian at the same temperature, at times A) initial condition; B) 0.10; C) 0.29; D) 0.48; and E) 0.67, in units of the thermal electron collision time τ_R.*

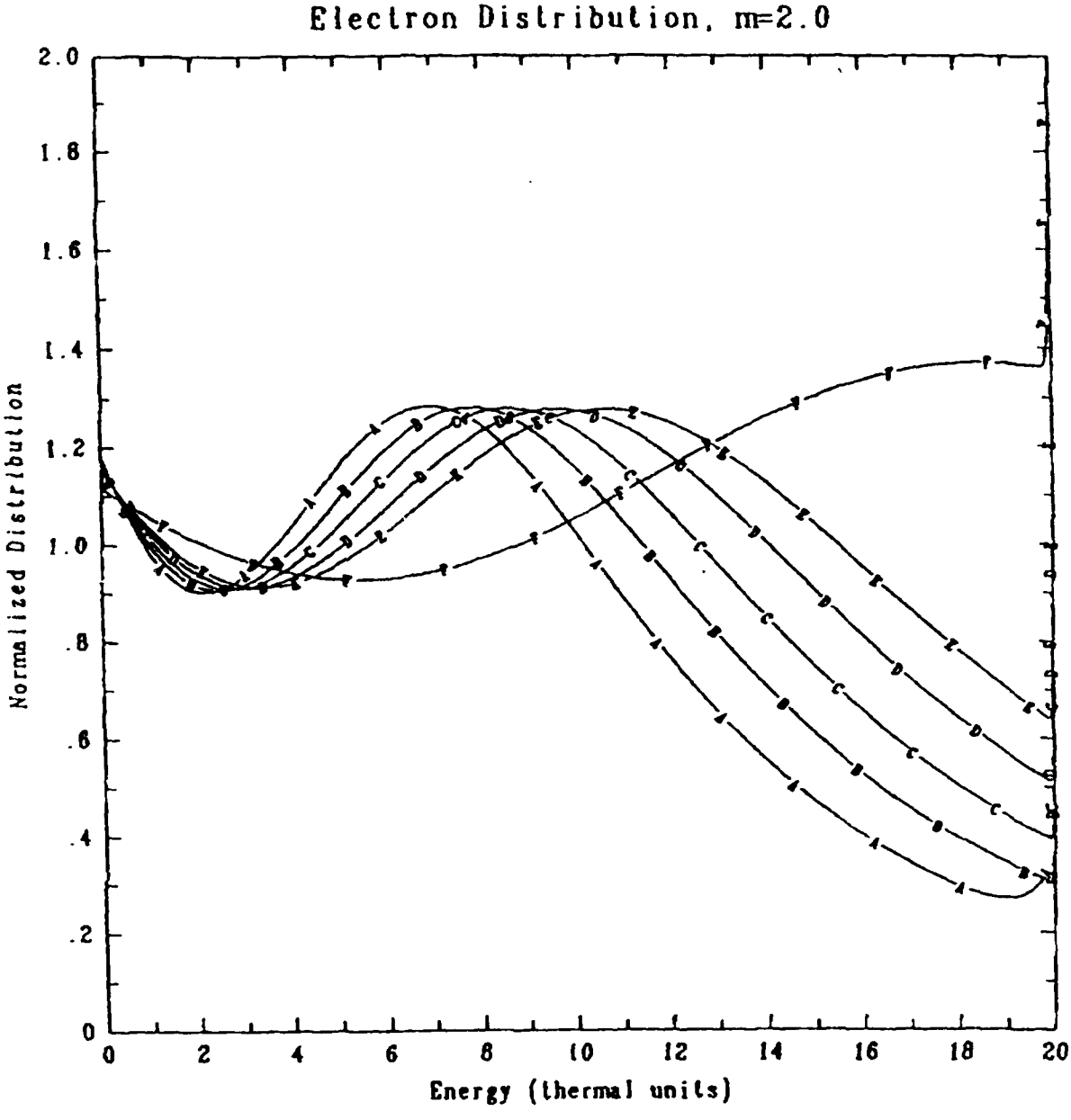

Figure 10. *Time-evolution of a distribution function from an ohmically-heated distribution under the influence of a constant compressional heating only. (Initial distribution is that of fig. (8) at* $\tau = 1.078$*). For this plot, the compression coefficient was set to* $\frac{2}{3}\tau_R \vec{\nabla} \cdot \vec{V} = 1$ *(see eq. (57)). The different curves correspond to times A) initial condition; B) 0.11; C) 0.21; D) 0.31; E) 0.41; and F) 0.92, in units of the thermal electron collision time* τ_R.

DISTRIBUTION LIST

Assistant to the Secretary of Defense Atomic Energy Washington, D.C. 20301 Attn: Executive Assistant	1 copy
Director Defense Nuclear Agency Washington, D.C. 20305	
Attn: DDST	1 copy
TITL	4 copies
RAEV	1 copy
STVI	1 copy
Commander Field Command Defense Nuclear Agency Kirtland AFB, New Mexico 87115 Attn: FCPR	1 copy
Director Joint Strat TGT Planning Staff Offutt AFB Omaha, Nebraska 68113 Attn: JLKS	1 copy
Undersecretary of Defense for RSCH and ENGRG Department of Defense Washington, D.C. 20301 Attn: Strategic and Space Systems (OS)	1 copy
Deputy Chief of Staff for RSCH DEV and ACQ Department of the Army Washington, D.C. 20301 Attn: DAMA-CSS-N	1 copy
Commander Harry Diamond Laboratories Department of the Army 2800 Powder Mill Road Adelphi, Maryland 20783 Attn: DELHD-N-NP DELHD-TA-L (Tech. Lib.)	1 copy each
U.S. Army Missile Command Redstone Scientific Information Center Attn: DRSMI-RPRD(Documents) Redstone Arsenal, Alabama 35809	3 copies
Commander U.S. Army Nuclear and Chemical Agency 7500 Backlick Road Building 2073 Springfield, Virginia 22150 Attn: Library	1 copy

Commander
Naval Intelligence Support Center
4301 Suitland Road, Bldg. 5
Washington, D.C. 20390
Attn: NISC-45

1 copy

Commander
Naval Weapons Center
China Lake, California 93555
Attn: Code 233 (Tech. Lib.)

1 copy

Officer in Charge
White Oak Laboratory
Naval Surface Weapons Center
Silver Spring, Maryland 20910
Attn: Code R40
Code F31

1 copy each

Weapons Laboratory
Kirtland AFB, New Mexico 87117-6008
Attn: Dr. William Baker
SUL
CA

1 copy each

Deputy Chief of Staff
Research, Development and Accounting
Department of the Air Force
Washington, D.C. 20330
Attn: AFRDQSM

1 copy

Commander
U.S. Army Test and Evaluation Command
Aberdeen Proving Ground, Maryland 21005
Attn: DRSTE-EL

1 copy

Auburn University
Department of Physics
Attn: Dr. J. Perez
Auburn, Al 36849

1 copy

BDM Corporation
7915 Jones Branch Drive
McLean, Virginia 22101
Attn: Corporate Library

1 copy

Berkeley Research Associates
Post Office Box 983
Berkeley, California 94701
Attn: Dr. Joseph Workman

1 copy

Berkeley Research Associates — 1 copy each
Post Office Box 852
5532 Hempstead Way
Springfield, Virginia 22151
Attn: Dr. Joseph Orens

Boeing Company — 1 Copy
Post Office Box 3707
Seattle, Washington 98134
Attn: Aerospace Library

General Electric Company - Tempo — 1 Copy
Center for Advanced Studies
816 State Street
Post Office Drawer QQ
Santa Barbara, California 93102
Attn: DASIAC

Institute for Defense Analyses — 1 copy
1801 N. Beauregard Street
Alexandria, Virginia 22311
Attn: Classified Library

JAYCOR — 1 copy
1608 Spring Hill Road
Vienna, Virginia 22180
Attn: R. Sullivan

JAYCOR — 1 copy
11011 Forreyane Road
Post Office Box 85154
San Diego, California 92138
Attn: E. Wenaas
F. Felber

KAMAN Sciences Corporation — 1 copy each
Post Office Box 7463
Colorado Springs, Colorado 80933
Attn: Library

Lawrence Livermore National Laboratory — 1 copy each
University of California
Post Office Box 808
Livermore, California 94550
Attn: DOC CDN for 94550
DOC DCN for L-47 L. Wouters
DOC CDN for Tech. Infor. Dept. Lib.

Lockheed Missiles and Space Company, Inc. — 1 copy each
Post Office Box 504
Sunnyvale, California 94086
Attn: S. Taimlty
J.D. Weisner

Maxwell Laboratory, Inc. — 1 copy ea.
9244 Balboa Avenue
San Diego, California 92123
Attn: A. Kolb
K. Ware

McDonnell Douglas Corporation — 1 copy
5301 Bolsa Avenue
Huntington Beach, California 92647
Attn: S. Schneider

Mission Research Corporation — 1 copy each
Post Office Drawer 719
Santa Barbara, California 93102
Attn: C. Longmire

Mission Research Corporation-San Diego — 1 copy
5434 Ruffin Road
San Diego, California 92123
Attn: Victor J. Van Lint

Northrop Corporation — 1 copy
Northrop Research & Technology Center
1 Research Park
Palos Verdes Peninsula, California 90274

Physics International Company — 1 copy each
2700 Merced Street
San Leandro, California 94577
Attn: C. Deeney
T. Nash

R and D Associates — 1 copy each
Post Office Box 9695
Marina Del Rey, California 90291
Attn: Library

Science Applications, Inc. — 1 copy
10260 Campus Point Drive
Mail Stop 47
San Diego, California 92121
Attn: R. Beyster

Science Research Laboratory
1150 Ballena Blvd., Suite 100
Alameda, California 94501
Attn: M. Krishnan

Spectra Technol, Inc., 1 copy
2755 Northup Way
Bellevue, Washington 98004
Attn: Alan Hoffman

Spire Corporation 1 copy
Post Office Box D
Bedford, Massachusetts 07130
Attn: R. Little

Director 1 copy
Strategic Defense Initiative Organization
Pentagon 20301-7100
Attn: T/IS Dr. Dwight Duston

Texas Tech University 1 copy
Post Office Box 5404
North College Station
Lubbock, Texas 79417
Attn: T. Simpson

TRW Defense and Space Systems Group 1 copy
One Space Park
Redondo Beach, California 90278
Attn: Technical Information Center

Naval Research Laboratory
Radiation Hydrodynamics Branch
Washington, D.C. 20375
Code 4720 - 50 copies
4700 - 26 copies
2628 - 22 copies

Do NOT make labels for
Records 1 cy

Director of Research 2 copies
U.S. Naval Academy
Annapolis, MD 21402

Naval Research Laboratory 1 copy
Washington, DC 20375-5000
Code 1220

Naval Research Laboratory 1 copy
Washington, DC 20375-5000
Code 4630
Timothy Calderwood